Chaos, Solitons and Fractals 176 (2023) 114143

Contents lists available at ScienceDirect

Chaos, Solitons and Fractals

journal homepage: www.elsevier.com/locate/chaos

A 2D piecewise-linear discontinuous map arising in stock market modeling: Two overlapping period-adding bifurcation structures

Laura Gardini [a], Davide Radi [b,c], Noemi Schmitt [d], Iryna Sushko [e,*], Frank Westerhoff [d]

[a] Department of Economics, Society and Politics, University of Urbino Carlo Bo, Italy
[b] Department of Finance, VŠB - Technical University of Ostrava, Ostrava, Czech Republic
[c] Department of DiMSEFA, Catholic University of Milan, Italy
[d] Department of Economics, University of Bamberg, Germany
[e] Institute of Mathematics, NASU, and Kyiv School of Economics, Kyiv, Ukraine

ARTICLE INFO

Keywords:
2D piecewise-linear discontinuous maps
Border-collision bifurcations
Period-adding bifurcation structure
Coexisting attractors
Center bifurcation
Stock market dynamics

ABSTRACT

We consider a 2D piecewise-linear discontinuous map defined on three partitions that drives the dynamics of a stock market model. This model is a modification of our previous model associated with a map defined on two partitions. In the present paper, we add more realistic assumptions with respect to the behavior of sentiment traders. Sentiment traders optimistically buy (pessimistically sell) a certain amount of stocks when the stock market is sufficiently rising (falling); otherwise they are inactive. As a result, the action of the price adjustment is represented by a map defined by three different functions, on three different partitions. This leads, in particular, to families of attracting cycles which are new with respect to those associated with a map defined on two partitions. We illustrate how to detect analytically the periodicity regions of these cycles considering the simplest cases of rotation number $1/n$, $n \geq 3$, and obtaining in explicit form the bifurcation boundaries of the corresponding regions. We show that in the parameter space, these regions form two different overlapping period-adding structures that issue from the center bifurcation line. In particular, each point of this line, associated with a rational rotation number, is an issue point for two different periodicity regions related to attracting cycles with the same rotation number but with different symbolic sequences. Since these regions overlap with each other and with the domain of a locally stable fixed point, a characteristic feature of the map is multistability, which we describe by considering the corresponding basins of attraction. Our results contribute to the development of the bifurcation theory for discontinuous maps, as well as to the understanding of the excessively volatile boom-bust nature of stock markets.

1. Introduction

For several decades, many researchers have been interested in the underlying mechanisms that lead to the wild behavior of stock markets, which repeatedly exhibit boom-bust cycles and are excessively volatile. The main role in such behavior is attributed to the presence of chartists and fundamentalists. Chartists are typically represented as traders who extrapolate stock price trends, while fundamental traders presume that stock prices will revert towards their fundamental values (see review articles [1,2]). The nonlinear interaction between these two types of trading philosophies has been shown in many contributions (among which we mention [3–5]), in particular, for models that are analytically tractable since they are represented by one-dimensional (1D) maps (e.g. in [6–8]). Recent works, [9] and [10], have introduced chartist-fundamentalist models associated with two-dimensional (2D) piecewise-linear maps, that allow a more detailed description of the behavior of stock market participants. See also [11] for a chartist-fundamentalist model that corresponds to a 2D piecewise-smooth map with nonlinear branches.

Our goal is to make the simplest assumptions leading to models that can be used to mimic the market dynamics. As a starting point, we take the stock market model proposed in [10], where market makers quote stock prices with respect to the order flow of chartists, fundamentalists, and sentiment traders (being subject to animal spirits). Chartists place buying (selling) orders when stock prices increase (decrease), whereas fundamentalists place buying (selling) orders when stock prices are low (high). The order sizes of chartists and fundamentalists are proportional to their trading signals. Sentiment traders optimistically buy a certain amount of stocks in rising stock markets and pessimistically sell a

* Corresponding author.
E-mail addresses: laura.gardini@uniurb.it (L. Gardini), davide.radi@unicatt.it (D. Radi), noemi.schmitt@uni-bamberg.de (N. Schmitt), sushko@imath.kiev.ua (I. Sushko), frank.westerhoff@uni-bamberg.de (F. Westerhoff).

https://doi.org/10.1016/j.chaos.2023.114143
Received 4 September 2023; Accepted 2 October 2023
Available online 12 October 2023

certain amount of stocks in falling markets. The dynamics of the related stock market model depends essentially on two partitions where the related 2D piecewise-linear discontinuous map has different definitions. The results obtained with that simple model were promising (as reported e.g. in [12]), but it lacked a region where fundamental equilibrium exists. To address this gap, in the present paper we propose and study a generalized version of the stock market model in [10], assuming that sentiment traders exhibit three types of behavior: they are optimistic and buy (are pessimistic and sell) a certain amount of stocks *only* when the stock market is sufficiently increasing (decreasing), and they are neutral and abstain from trading when the stock market is relatively stable. This simple and realistic assumption strongly affects the dynamics of the model which is now determined by a 2D piecewise-linear discontinuous map defined by three different functions on three different partitions.

Recall that piecewise-smooth dynamical systems have been considered by many researchers not only from a theoretical point of view, but also with respect to a wide range of applications of these systems in various fields (see, e.g., [13–15]). In particular, in economics and finance many models have been proposed that are ultimately described by piecewise-smooth maps (besides the papers mentioned above, see also [16]). These maps are characterized by the existence of border(s), often called switching manifolds, at which the system changes its definition. As a result, under parameter variation one can observe not only the bifurcations typical for smooth systems, but also so-called border-collision bifurcations[1] (BCBs for short). The bifurcation theory of nonsmooth systems is more developed for 1D and 2D continuous maps due to the related border-collision normal forms. As for discontinuous maps, many results have already been obtained for 1D maps (see [19] and references therein), while the bifurcations occurring in two- or higher-dimensional maps belong to a quite novel research field. To cite a few contributions related to a 2D map with one discontinuity line we refer to [20–22]. One of the aims of our work is therefore to describe new properties that are characteristic of 2D discontinuous maps.

As mentioned above, the dynamics of the stock market model under consideration are determined by a 2D piecewise-linear map defined on three partitions that are separated by two discontinuity lines. A specific property of this map is that the Jacobian matrix is the same in all the partitions, which facilitates obtaining analytical results. Since the standard local bifurcations occurring in smooth maps cannot occur in piecewise-linear maps, the main role in determining the existence and bifurcations of various invariant sets of the map is associated with BCBs. In particular, an n-cycle may disappear/appear due to a BCB occurring when a periodic point has a contact with one of the discontinuity lines.

In the present paper, we derive explicit expressions for BCB curves bounding periodicity regions of attracting n-cycles with rotation number[2] $1/n$, $n \geq 3$. Economically, this does not only mean that we can rigorously prove that our modeling of animal spirits may generate excessively volatile boom-bust dynamics, but also that we can analytically characterize how the behavior of different trader types affects the dynamics of stock markets. In doing so, we also describe new bifurcation structures that, to the best of our knowledge, have not been observed in other maps. Namely, we determine two different kinds of families of cycles: the first kind includes families of cycles with points in two partitions only, while families of the second kind include cycles with points in all three partitions. In the parameter space, the corresponding periodicity regions form two different overlapping period-adding structures[3] issuing from the line related to the center bifurcation of the fixed point. Specifically, from each point of the center bifurcation line, corresponding to a rational rotation number, two periodicity regions are issuing related to attracting cycles with the same rotation number but with different symbolic sequences. For a description of a period-adding bifurcation structure, we refer to [19]; for the center bifurcation, see [25].

Our analysis also shows that a locally stable fixed point, at which the stock price matches its fundamental value, mainly coexists with other attracting cycles whose points are located around the fundamental value. When the stock market is hit by exogenous shocks, coexisting attractors may yield interesting attractor-switching dynamics, such as alternating periods between fixed point and cyclical motion. In this respect, knowledge of the properties of the basins of attraction, e.g., how the behavior of certain trader types affects their size, is important from an economic policy perspective, and we show how to derive the basin boundaries.

Our paper is organized as follows. In Section 2, we present a generalized version of the stock market model proposed in [10]. In Section 3, we outline a number of preliminary properties, including a description of the so-called stability box related to an attracting (fundamental) fixed point, which may coexist with one or several attracting cycles. A mechanism of creation of these cycles can be explained as follows: among the fixed points of the linear components of the map, only one (fundamental) fixed point is actual while two other fixed points are virtual; however, these virtual fixed points play the role of "ghosts" influencing the overall dynamics by forcing the trajectories to jump between the different partitions and eventually create various cycles. We also discuss the role of the discontinuity lines, as well as their images and preimages. Since the considered discontinuous map is invertible, it represents a two-dimensional analog of a gap-map (occurring in the theory of 1D piecewise linear maps [26]). Our main results are presented in Section 4. First, we show that a 2-cycle exists (being unique) only outside the stability box, where all other cycles are saddles. We obtain the two conditions associated with the first homoclinic bifurcation of this 2-cycle, which determines the boundaries of the parameter region associated with chaotic attractors. The attracting chaotic sets have the structure of those occurring in a Belykh map (see [27]), belonging to a region in the phase space in which all cycles are saddles, existing when the 2−cycle is not homoclinic. Then we show that for parameters belonging to the stability box, a locally attracting fixed point may coexist with one or several attracting cycles. In particular, we detect the BCB boundaries of the periodicity regions related to attracting cycles with rotation number $1/n$, $n \geq 3$, belonging to two different kinds of families, as mentioned above, namely, with points in two outermost partitions only and with points in all three partitions. We present numerical evidence that the corresponding periodicity regions are organized in two different period-adding bifurcation structures issuing from the center bifurcation line. With respect to the center bifurcation, we show the existence of an invariant polygon or an invariant ellipse (associated with a rational or irrational rotation number, respectively) filled with periodic or quasiperiodic trajectories. Some conclusions are drawn in Section 5.

2. A generalized stock market model

In this section, we first generalize the stock market model proposed in [10] and then derive the map that governs its dynamics. The main

[1] This notation was introduced by Nusse and Yorke in [17] (see also [18]).

[2] In the case considered, the unique fixed point of the map is a focus, and we consider n-cycles with points located around this fixed point. In simpler terms, the rotation number of such a cycle is an irreducible fraction m/n, where m is the number of rotations of the trajectory around the fixed point in n iterations. For a rigorous definition, see, e.g., [23].

[3] In [24] a model is considered whose dynamics is determined by a 2D piecewise-linear map defined on four partitions separated by two discontinuity lines. It also shows the existence of several overlapping not *period-adding* but *period-incrementing* bifurcation structures. See [19] for a description of these two bifurcation structures.

difference between our two stock market models is that, due to a no-trade zone for sentiment traders, the number of partitions on which the map is defined increases from two to three, leading to novelties in the dynamic scenarios that can be observed.

2.1. Model setup

Four types of market participants populate the stock market model that we consider in our paper: market makers, chartists, fundamentalists, and sentiment traders. Let us start with the behavior of market makers. Market makers change the stock price from period t to period $t+1$ with respect to current excess demand. To be precise, they periodically quote new stock prices using the linear price-adjustment rule

$$P_{t+1} = P_t + a(D_t^C + D_t^F + D_t^S), \tag{1}$$

where parameter $a > 0$ denotes the strength with which market makers adjust the current stock price with respect to the orders of chartists, fundamentalists, and sentiment traders, given by D_t^C, D_t^F, and D_t^S, respectively. Market makers increase (decrease) the stock price accordingly when confronted with excess buying (selling).

Since chartists seek to exploit stock price trends, they place buying orders when the stock market is rising and selling orders when the stock market is falling. We formalize their trading behavior as

$$D_t^C = b(P_t - P_{t-1}), \quad b > 0. \tag{2}$$

Note that the size of the orders placed by chartists depends on the strength of their technical trading signal, given by the current stock price trend, and their general aggressiveness, represented by parameter b.

Fundamental analysis rests on the assumption that the stock price will return towards its fundamental value. Fundamentalists place buying orders when the stock market is undervalued and selling orders when the stock market is overvalued. Let F stand for the stock market's fundamental value. Since fundamentalists follow the trading rule

$$D_t^F = c(F - P_t), \quad c > 0, \tag{3}$$

the size of their orders depends on the strength of their fundamental trading signal, given by the stock market's current mispricing, and their general aggressiveness, captured by parameter c.

Sentiment traders are subject to Keynesian animal spirits. According to Keynes, [28], human agents recurrently show collective, (apparently) spontaneous, and significant shifts in their sentiment, say a transition from pessimism to optimism, upon which they act. In this paper, we consider the case where sentiment traders display three distinct moods. Sentiment traders are either optimistic, pessimistic, or neutral, depending on whether stock prices are sufficiently increasing, sufficiently decreasing, or relatively stable. Moreover, sentiment traders' mood affects their trading behavior, which we express as

$$D_t^S = \begin{cases} d & \text{if} \quad P_t - P_{t-1} > h, \\ 0 & \text{if} \quad -h \le P_t - P_{t-1} \le h, \\ -d & \text{if} \quad P_t - P_{t-1} < -h, \end{cases} \qquad d > h > 0. \tag{4}$$

Parameter d reflects the number of stocks sentiment traders are willing to trade in a given period. Parameter h controls under which stock market conditions sentiment traders are optimistic, pessimistic, or neutral. To be more precise, sentiment traders optimistically buy d units of stock when the stock market increases by more than h ($P_t - P_{t-1} > h$) and pessimistically sell d units of stock when the stock market decreases by more than h ($P_t - P_{t-1} < -h$). When the stock market is relatively stable, i.e., when stock price changes are bounded between the two values, $-h \le P_t - P_{t-1} \le h$, sentiment traders' mood is neutral and they do not trade.

A remark with respect to the behavior of sentiment traders is in order. In [10], it is considered the case $d > 0$ and $h = 0$, resulting in a stock market model with two generic sentiment states, i.e., optimism and pessimism, and one nongeneric sentiment state, namely neutral. By considering three generic sentiment states, one may deem our setup more general. In fact, human agents are not always optimistic or pessimistic. To understand the transition from two to three generic sentiment states, our main attention will be on the case $d > h > 0$, i.e., we consider that parameter h transgresses from zero into the positive domain. Needless to say, for $h = d = 0$, sentiment traders vanish from our stock market model. We then end up with a linear chartist-fundamentalist model, which serves us as a useful benchmark.

2.2. Dynamic model

Given the behavior of the four market participants, we can now derive the law of motion of our stock market model. Inserting (2), (3), and (4) into (1) and rearranging terms, we find that the stock price in period $t+1$ adheres to

$$P_{t+1} = \begin{cases} P_t + a(b(P_t - P_{t-1}) + c(F - P_t) + d) & \text{if} \quad P_t - P_{t-1} > h, \\ P_t + a(b(P_t - P_{t-1}) + c(F - P_t)) & \text{if} \quad -h \le P_t - P_{t-1} \le h, \\ P_t + a(b(P_t - P_{t-1}) + c(F - P_t) - d) & \text{if} \quad P_t - P_{t-1} < -h. \end{cases} \tag{5}$$

Note that the parameters ab, ac, and ad reflect the model impact of chartists, fundamentalists, and sentiment traders, which we rename for convenience as b, c, and d, respectively. Furthermore, it is convenient to express our generalized stock market model in deviation from the fundamental value. Defining $P_t := P_t - F$ yields

$$P_{t+1} = \begin{cases} P_t + b(P_t - P_{t-1}) - cP_t + d & \text{if} \quad P_t - P_{t-1} > h, \\ P_t + b(P_t - P_{t-1}) - cP_t & \text{if} \quad -h \le P_t - P_{t-1} \le h, \\ P_t + b(P_t - P_{t-1}) - cP_t - d & \text{if} \quad P_t - P_{t-1} < -h. \end{cases} \tag{6}$$

Introducing the auxiliary variable $X_t = P_{t-1}$, we arrive at the two-dimensional piecewise-linear discontinuous map:

$$T : \begin{cases} P_{t+1} = \begin{cases} (1+b-c)P_t - bX_t + d & \text{if } P_t - X_t > h, \\ (1+b-c)P_t - bX_t & \text{if } -h \le P_t - X_t \le h, \\ (1+b-c)P_t - bX_t - d & \text{if } P_t - X_t < -h, \end{cases} \\ X_{t+1} = P_t. \end{cases} \tag{7}$$

In the absence of sentiment traders, the above map simplifies to

$$T_O : \begin{cases} P_{t+1} = (1+b-c)P_t - bX_t, \\ X_{t+1} = P_t, \end{cases} \tag{8}$$

whose unique fixed point is obviously given by the origin, representing the stock market's fundamental value. In this elementary chartist-fundamentalist model, a two-dimensional linear map drives the dynamics of the stock price. Clearly, the differences we see in the properties of maps T and T_O are entirely due to the behavior of sentiment traders.

Denoting the variables as $x_t := P_t$ and $y_t := X_t$ and skipping the time index, map T can be written as follows:

$$T = \begin{cases} T_L : \begin{pmatrix} x \\ y \end{pmatrix} \\ \quad \to J \begin{pmatrix} x \\ y \end{pmatrix} + \begin{pmatrix} d \\ 0 \end{pmatrix} \text{ if } (x,y) \in D_L = \{(x,y) : y < x - h\}, \\ T_O : \begin{pmatrix} x \\ y \end{pmatrix} \\ \quad \to J \begin{pmatrix} x \\ y \end{pmatrix} \text{ if } (x,y) \in D_O = \{(x,y) : x - h < y < x + h\}, \\ T_U : \begin{pmatrix} x \\ y \end{pmatrix} \\ \quad \to J \begin{pmatrix} x \\ y \end{pmatrix} - \begin{pmatrix} d \\ 0 \end{pmatrix} \text{ if } (x,y) \in D_U = \{(x,y) : y > x + h\}, \end{cases}$$

(9)

where J is the Jacobian matrix given by

$$J = \begin{pmatrix} v & -b \\ 1 & 0 \end{pmatrix}, \; v = 1 + b - c. \tag{10}$$

Note that index L in map T refers to the lower partition with respect to the straight line $y = x - h$, index U refers to the upper partition with respect to the straight line $y = x + h$, and index O refers to the strip between these two straight lines. Furthermore, rescaling $x := x/d$ or $x := x/h$ (and similarly for y) allows us to set $d = 1$ or $h = 1$, respectively. However, due to their economic role, we prefer to keep both these parameters in our mathematical analysis. As already mentioned, our main focus will be on the case $d > h > 0$. Unless otherwise stated, we fix $d = 0.02$ and $h = 0.01$ in our numerical analysis.

3. Preliminary remarks, definitions, and basins of attraction

In Section 3.1, we present some general properties of map T. In Section 3.2, we introduce the critical lines (the discontinuity lines) and describe some related properties. In fact, not only the discontinuity lines but also their forward and backward iterations are relevant. Considering the images, we obtain the boundaries of regions of the phase plane that cannot include any periodic point, while the preimages determine segments belonging to the boundaries of the basins of attraction of different coexisting attracting cycles. We also introduce the symbolic representation of cycles.

3.1. General properties of map T

The properties we discuss in the following also hold, with some minor differences, for the maps studied in [10] and [12], i.e., for the case $h = 0$ associated with a map defined on two partitions.

• (Symmetry) Map T is symmetric with respect to the origin. The proof is straightforward. Since $T_O(-x,-y) = -T_O(x,y)$ and $T_U(-x,-y) = -T_L(x,y)$, it follows that the trajectory of a point $(-x_0,-y_0)$ is symmetric with respect to the origin to the trajectory of the point (x_0,y_0). From this property, we have that any invariant set of map T is either symmetric with respect to the origin, or its symmetric set with respect to the origin is also invariant.

• (Fixed points) The fixed point $P_O = (0,0)$ of map T_O is the unique actual fixed point of map T. The fixed points $P_L = (d/c, d/c)$ and $P_U = (-d/c, -d/c)$ of maps T_L and T_U belong to the diagonal, where map T_O is defined, so that they are virtual for map T, denoted as $\overline{P}_L$ and $\overline{P}_U$.

• (Eigenvalues of J and stability box S) The Jacobian matrix J is the same in all three partitions, with determinant $\det J = b$ and trace $trJ = v$. In the (b,c)-parameter plane of interest, with $b > 0$ and $c > 0$, the eigenvalues of the Jacobian matrix J, given by

$$\lambda_{1,2} = 0.5(v \pm \sqrt{v^2 - 4b}), \; v = 1 + b - c, \tag{11}$$

satisfy $|\lambda_{1,2}| < 1$ in region S called *the stability box,*

$$S = \{(b,c) : 0 < b < 1, 0 < c < 2(1+b)\}, \tag{12}$$

shown in yellow in Fig. 1a, which includes three regions: $R_1 = \{(b,c) : 0 < b < 1, 1 + b - 2\sqrt{b} < c < 1 + b + 2\sqrt{b}\}$, $R_2 = \{(b,c) : 0 < b < 1, 0 < c \le 1 + b - 2\sqrt{b}\}$, and $R_3 = \{(b,c) : 0 < b < 1, +b - 2\sqrt{b} \le c < 2(1+b)\}$, related to complex conjugate, real positive, and real negative eigenvalues, respectively. Since the Jacobian matrix J is the same in all three partitions of map T, for $(b,c) \in S$, not only the fixed point P_O but also all the existing cycles are *attracting*. However, we shall see that an attracting 2-cycle does not exist, so that this holds for all n-cycles of period $n \ge 3$. The fixed point P_O undergoes a *degenerate flip* bifurcation (see [29]) at the border $b = 2(1 + c)$ of S, and a *center* bifurcation (see [25]) at the border $b = 1$ of S.

• (Parameter region R_4) For $(b,c) \in R_4 = \{(b,c) : 0 < b < 1, c > 2(1+b)\}$, the eigenvalues of J are $-1 < \lambda_1 < 0$ and $\lambda_2 < -1$, so that the fixed point P_O is a saddle, and all the cycles of map T are saddles as well because the eigenvalues of J^n associated with a cycle of period $n \ge 1$ satisfy $-1 < \lambda_1^n < 0$, $\lambda_2^n < -1$ for odd n, and $0 < \lambda_1^n < 1$, $\lambda_2^n > 1$ for even n. However, this does not necessarily imply divergent dynamics (as it occurs for a generic trajectory when the map is defined only via map T_O), because chaotic attractors may exist, leading to bounded dynamics with humped behaviors of stock prices.

In the absence of sentiment traders, the dynamics of our stock market model depend only on map T_O, and the stability box S corresponds to the parameter region where the fixed point P_O is globally attracting. For map T, however, the stability box S corresponds to the parameter region where the fixed point P_O is locally attracting. Depending on whether parameters b and c are located in regions R_1, R_2, or R_3, locally we observe either a cyclical, a monotonic, or an alternating convergence of the stock price towards its fundamental value. In fact, the difference between the trivial dynamics of map T_O and the piecewise-linear discontinuous map T leads to the coexistence of the locally stable fundamental fixed point with other stable cycles of various periods, surrounding P_O. As we will see, the basin of attraction of P_O depends on the width of the strip in which map T_O is defined, given by two segments on the discontinuity lines and related preimages.

Recall that in the case $h = 0$ (see [10] and [12]), the only region related to trajectories convergent to a fixed point is region R_2, which is either the virtual fixed point $\overline{P}_L$ or $\overline{P}_U$, both attracting in the Milnor sense [30]. Put differently, in the case $h > 0$, for parameters belonging to the stability box S, map T has the locally attracting fundamental fixed point P_O, which may coexist with attracting cycles of different periods surrounding it. Some of the related periodicity regions in the (b,c)-parameter plane, obtained numerically, are shown in Fig. 1b for $n \le 40$. These regions issue from the center bifurcation line defined by $b = 1, 0 < c < 4$, corresponding to complex conjugate eigenvalues on the unit circle of the Jacobian matrix J, and the boundaries of these regions are BCB curves. In Section 4, we obtain analytically the boundaries of the largest periodicity regions corresponding to attracting n-cycles with rotation number $1/n$. But let us first introduce several notations related to the three partitions of the map, and describe some properties characteristic for the discontinuous case.

3.2. Critical lines of map T and their role

For piecewise smooth maps, weather continuous or discontinuous, the border at which the map changes its definition is called a *critical line* (following [31]). In fact, several properties of the dynamics of map T are related to these sets as well as to their images and preimages, also called critical lines of different ranks. In particular, it is known that in piecewise-linear discontinuous maps, the borders of the basins of attraction of coexisting attractors, besides stable invariant sets of saddle cycles, may be associated with preimages of the critical lines. A few examples are given below.

In our case, there are two critical lines of rank −1, denoted by $C_{-1,L}$ and $C_{-1,U}$:

$$C_{-1,L} = \{(x,y) : y = x - h\}, \quad C_{-1,U} = \{(x,y) : y = x + h\}. \tag{13}$$

For each critical line, we have to consider two images by the maps defined on the two different sides of the set:

$$\begin{aligned} C_L &= T_L(C_{-1,L}) = \left\{(x,y) : y = \tfrac{x}{1-c} - \tfrac{bh+d}{1-c}\right\}, \\ C_{O,L} &= T_O(C_{-1,L}) = \left\{(x,y) : y = \tfrac{x}{1-c} - \tfrac{bh}{1-c}\right\}, \\ C_U &= T_U(C_{-1,U}) = \left\{(x,y) : y = \tfrac{x}{1-c} + \tfrac{bh+d}{1-c}\right\}, \\ C_{O,U} &= T_O(C_{-1,U}) = \left\{(x,y) : y = \tfrac{x}{1-c} + \tfrac{bh}{1-c}\right\}. \end{aligned} \tag{14}$$

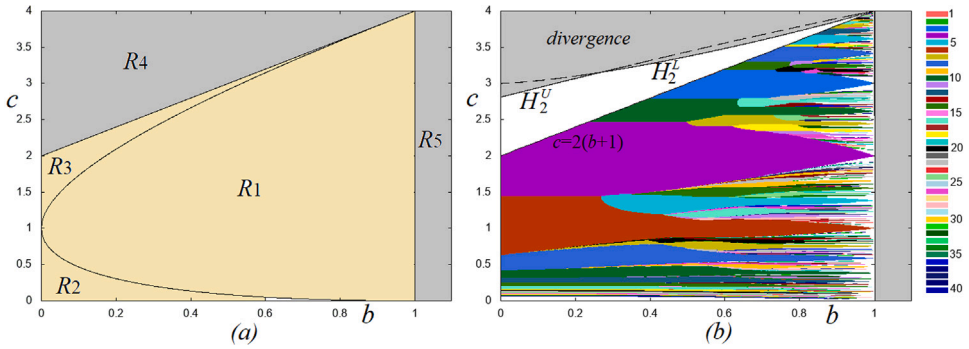

Fig. 1. In (a), stability box $S = R_1 \cup R_2 \cup R_3$ in the (b, c)-parameter plane. Region R_1 is characterized by complex eigenvalues, while region R_2 (R_3) is characterized by real and positive (real and negative) eigenvalues. In region R_4, the eigenvalues satisfy $-1 < \lambda_1 < 0$, $\lambda_2 < -1$, and all the existing cycles of map T are saddles. In region R_5, the eigenvalues are complex conjugate and larger than 1 in modulus. In (b), regions of different colors, obtained numerically, denote the existence of attracting n-cycles of different periods, $3 \le n \le 40$. The white region denotes the existence of a chaotic attractor, while the gray region denotes divergence. The remaining parameters are $h = 0.01$, $d = 0.02$.

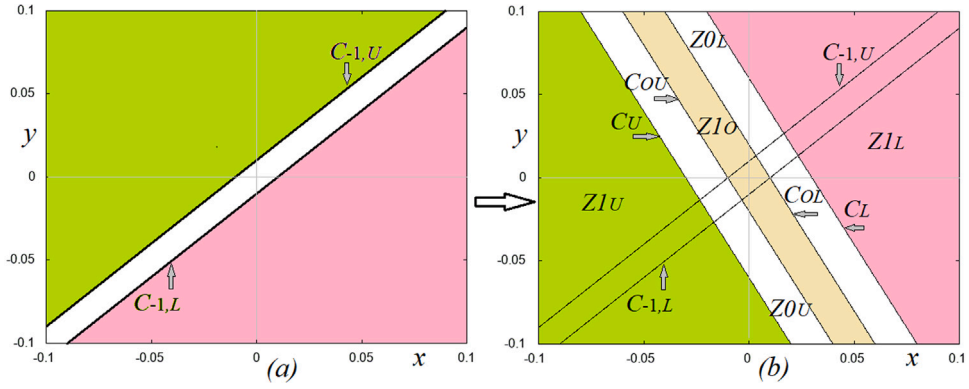

Fig. 2. (a) shows critical lines of map T, and (b) shows their images separating the regions whose points have one preimage ($Z1_U$, $Z1_L$, $Z1_O$) and no preimages ($Z0_L$, $Z0_U$). Here $b = 1$, $c = 1.5$, $h = 0.01$, $d = 0.02$.

All these lines have the same slope, given by $s = \frac{1}{1-c}$, $c \neq 1$. This slope is negative for $c > 1$ and positive for $0 < c < 1$ (see, e.g. Fig. 2, where $c = 1.5$).

Since the Jacobian matrix J is the same in all three partitions, the region of the phase plane on the right side of the straight line $C_{-1,L}$ is mapped by T_L on the right side of the line $C_L = T_L(C_{-1,L})$ (pink region denoted by $Z1_L$ in Fig. 2b), the region on the left side of the straight line $C_{-1,U}$ is mapped by T_U on the left side of the line $C_U = T_U(C_{-1,U})$ (green region $Z1_U$ in Fig. 2b), while the strip between $C_{-1,L}$ and $C_{-1,U}$ is mapped by T_O onto the strip between $C_{O,L}$ and $C_{O,U}$ (yellow region $Z1_O$ in Fig. 2b). It follows that there are two regions, $Z0_L$ and $Z0_U$ (see Fig. 2b), that cannot be reached by a trajectory, since no point of the phase plane can be mapped by T in these regions.

As a result, map T is an invertible map of the following type: the phase plane is divided into five regions, namely, regions $Z1_L$, $Z1_U$ and $Z1_O$, whose points have one preimage by T_L^{-1}, T_U^{-1} and T_O^{-1}, respectively; these regions are separated by two regions, $Z0_L$ and $Z0_U$, whose points have no rank−1 preimage. Moreover, since either no preimage or a unique preimage exists, sets $T^k(Z0_L)$ and $T^k(Z0_U)$ never intersect for any $k > 0$. A periodic point cannot belong to regions $Z0_L$ and $Z0_U$ (since points in these regions cannot have a preimage), and similarly any invariant set cannot have a point in these regions. Hence, neither a cycle nor an invariant set can have points belonging to the images of these strips. In fact, reasoning by contradiction, let us suppose that there exists a point p (not critical) of an invariant set $\mathcal{A}$ that belongs to $T^k(Z0_L)$ or $T^k(Z0_U)$ for some k. Since $\mathcal{A}$ is invariant (i.e., $T(\mathcal{A}) = \mathcal{A}$), each point of $\mathcal{A}$ has an infinite sequence of preimages in $\mathcal{A}$. However, this leads to a contradiction because if, for example, $p \in T^k(Z0_L)$, then $T^{-k}(p) \in Z0_L$ and a point in $Z0_L$ has no other preimages (similarly for $T^k(Z0_U)$).

To summarize, we can state the following property of set $\Omega = \mathbb{R}^2 \setminus \cup_{k\ge 0} T^k(Z0_L \cup Z0_U)$:

Property 1 (*Invertibility of Map T and Set Ω*). *For the feasible parameter range $b > 0$, $c > 0$,*

(i) map T is invertible; points of strip $Z0_L$ between the critical lines $C_{O,L}$ and C_L, and strip $Z0_U$ between the critical lines $C_{O,U}$ and C_U have no rank-1 preimage; all the other points have one rank-1 preimage;

(ii) any n-cycle of map T of any period $n \ge 1$, as well as any other invariant set, must belong to set Ω.

Clearly, the points belonging to $T^k(Z0_L)$ and $T^k(Z0_U)$ tend towards some attracting sets, at a finite distance or at infinity. That is, the ω-limit set of any trajectory of map T belongs to set Ω. In contrast to 1D piecewise-linear maps with a similar property (also known as gap maps, see [19,26], where only one attracting cycle can exist and chaos cannot occur), set Ω may include coexisting attracting cycles of different periods or attracting chaotic sets.

To represent a cycle $\{(x_i, y_i)\}_{i=0}^{n-1}$ of map T, we use its symbolic sequence $\sigma_0\sigma_1 \ldots \sigma_{n-1}$, where

$$\sigma_i = \begin{cases} L & \text{if } (x_i, y_i) \in D_L, \\ O & \text{if } (x_i, y_i) \in D_O, \\ U & \text{if } (x_i, y_i) \in D_U. \end{cases}$$

For short, we denote a cycle by its symbolic sequence. In Fig. 3a, for example, the attracting fixed point P_O coexists with two 4-cycles, L^2U^2 and $LOUO$, while in Fig. 3b P_O coexists with one 4-cycle $LOUO$, four 3-cycles, L^2U, U^2L, LOU, UOL, and one 10-cycle L^2UOLU^2LOU. Note that the symbolic sequence of a generic cycle consists of symbols L, O, and U, while in a nongeneric case, for a periodic point belonging

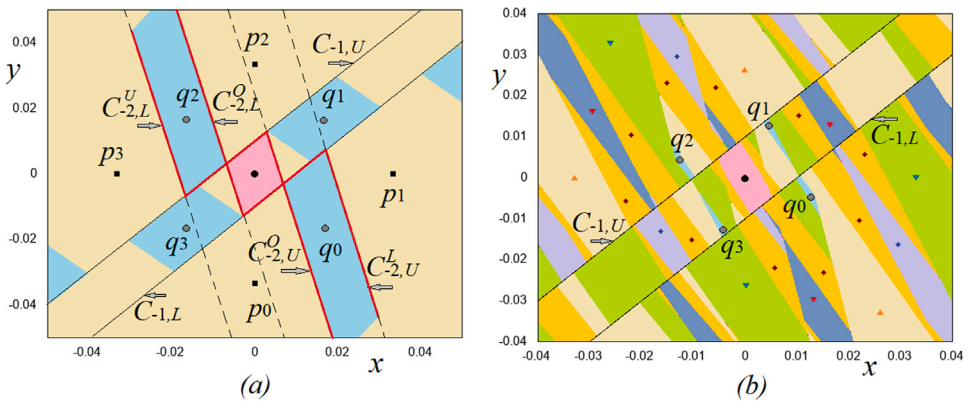

Fig. 3. Basins of attraction of the fundamental fixed point P_O coexisting with (a) two 4-cycles; (b) one 4-cycle, four 3-cycles, and one 10-cycle. Here, $h = 0.01$, $d = 0.02$, and (a) $b = 0.4$, $c = 2$; (b) $b = 0.5$, $c = 2.9$.

to the critical line $C_{-1,L}$ or $C_{-1,U}$, a special symbol can be introduced (say, B_L and B_U, respectively), and the presence of such a symbol in the symbolic sequence indicates that a BCB occurs. This occurs when, under parameter variation, a periodic point approaches border $C_{-1,L}$ or $C_{-1,U}$ from the inner part of strip D_O (where map T_O applies) or from region D_L or D_R (where map T_L or map T_U applies).

Let us discuss how basin boundaries of coexisting attractors can be determined. As already mentioned, for parameters belonging to the stability box S, in case of the coexistence of attracting sets, the basin boundaries cannot be associated with stable invariant sets of saddle cycles (they do not exist for $(a, b) \in S$). Instead, the basin boundaries are formed by segments of the critical lines $C_{-1,L}$, $C_{-1,U}$ and their preimages of different ranks. We can define the preimages of the critical lines $C_{-1,L}$ and $C_{-1,U}$ of rank−1 via three different linear maps. The preimages of $C_{-1,L}$ by T_O^{-1}, T_L^{-1}, and T_U^{-1} are denoted by $C^O_{-2,L}$ $C^L_{-2,L}$, and $C^U_{-2,L}$, respectively:

$$C^O_{-2,L} = T_O^{-1}(C_{-1,L}) = \left\{(x,y) : y = \left(1 - \frac{c}{b}\right)x - \frac{h}{b}\right\},$$
$$C^L_{-2,L} = T_L^{-1}(C_{-1,L}) = \left\{(x,y) : y = \left(1 - \frac{c}{b}\right)x - \frac{h+d}{b}\right\},$$
$$C^U_{-2,L} = T_U^{-1}(C_{-1,L}) = \left\{(x,y) : y = \left(1 - \frac{c}{b}\right)x - \frac{h-d}{b}\right\},$$

and the preimages of $C_{-1,U}$ are denoted by $C^O_{-2,U}$, $C^L_{-2,U}$, and $C^U_{-2,U}$, respectively:

$$C^O_{-2,U} = T_O^{-1}(C_{-1,U}) = \left\{(x,y) : y = \left(1 - \frac{c}{b}\right)x + \frac{h}{b}\right\},$$
$$C^L_{-2,U} = T_L^{-1}(C_{-1,U}) = \left\{(x,y) : y = \left(1 - \frac{c}{b}\right)x + \frac{h+d}{b}\right\},$$
$$C^U_{-2,U} = T_U^{-1}(C_{-1,U}) = \left\{(x,y) : y = \left(1 - \frac{c}{b}\right)x + \frac{h-d}{b}\right\}.$$

The basin boundaries of the coexisting attractors include segments of these straight lines. In Fig. 3a, for example, two segments of the critical lines $C_{-1,L}$ and $C_{-1,U}$, and two segments of the rank−1 preimages $C^O_{-2,L}$ and $C^O_{-2,U}$ bound the basin of attraction of the fixed point P_O, while different segments of $C_{-1,L}$, $C_{-1,U}$ and segments of four rank-1 preimages $C^O_{-2,L}$, $C^O_{-2,U}$, $C^L_{-2,L}$, and $C^L_{-2,U}$ belong to the basin boundaries of two attracting 4-cycles, L^2U^2 and $LOUO$.

As we can see, map T can have an attracting cycle of even period with points belonging to D_L and D_U only, similar to the case $h = 0$ described in [12]. For $h > 0$, however, a cycle of the same even period may also exist with periodic points belonging to three different regions, D_L, D_O, and D_U, that is, a cycle with symbolic sequence containing symbols L, U, and O (see Fig. 3a, where two 4-cycles have symbolic sequences L^2U^2 and $LOUO$, and Fig. 3b, where four different 3-cycles are shown).

It is worth noting that the coexistence of several attracting cycles with the attracting fixed point P_O occurs not only for $(b, c) \in R_1$, related to complex conjugate eigenvalues of the Jacobian matrix J. As can be seen in Fig. 1b, it holds also for $(b, c) \in R_2$, associated with real and positive eigenvalues of J. This is a new property related to three partitions of the map and to the fact that the fixed point P_O always exists. Put differently, when the map is defined on two partitions, for $h = 0$ and $(b, c) \in R_2$, map T has two virtual fixed points that are Milnor attractors, and no other attracting set can exist. Moreover, the coexistence of two different cycles, besides P_O, in region R_2 is also possible, as shown in Fig. 4a.

4. Main results

This section contains our main results. In Section 4.1, we introduce two kinds of families of cycles that are of interest, and state a useful property with respect to the stability of all possible cycles of map T. In Section 4.2, we explore the relation between the 2-cycle LU and the existence of chaotic attractors. In Sections 4.3 to 4.6, we describe the bifurcation structures in the (b, c)-parameter plane. In Section 4.7, we show that the periodicity regions related to attracting cycles of two different structures are issuing from particular bifurcation points.

4.1. Two kinds of families of cycles and their stability

Due to the symmetry with respect to the origin (see Section 3.1), any n-cycle, $n \geq 2$, of map T is either symmetric itself, or one more symmetric n-cycle exists. In all the considerations below, we assume that the rotation number of an n-cycle is $1/n$. Obviously, a cycle of *even* period n may be symmetric with respect to the origin. If a cycle has no points in partition D_O and m points in each partition D_L and D_U, then its symbolic sequence is L^mU^m, $n = 2m$, $m \geq 1$, and due to the linearity of maps T_L and T_U, this cycle is unique (see, e.g., cycle L^2U^2 in Fig. 3a). As we have already seen, map T can have a cycle of even period with periodic points also in partition D_O, and due to the symmetry, in D_O there must be at least two periodic points of the same cycle. In the simplest case, there are exactly two periodic points in D_O, so that the symbolic sequence of such an n-cycle of even period is L^mOU^mO, $n = 2m + 2$, $m \geq 1$ (see, e.g., cycle $LOUO$ in Fig. 3a).

In contrast, a cycle of *odd* period n cannot be symmetric with respect to the origin, and it necessarily coexists with a symmetric cycle of the same period. In the simplest case, if an odd-period cycle has no points in D_O, then two related symmetric cycles are L^mU^{m-1} and U^mL^{m-1}, $n = 2m - 1$, $m \geq 2$ (see, e.g., cycles L^2U and U^2L in Fig. 3b). Map T can also have an odd-period cycle with points in D_O. Again, in the simplest case, a couple of such cycles have symbolic sequences L^mOU^m, U^mOL^m, $n = 2m + 1$, $m \geq 1$, each with one point in D_O (see, e.g., cycles LOU and UOL in Fig. 3b).

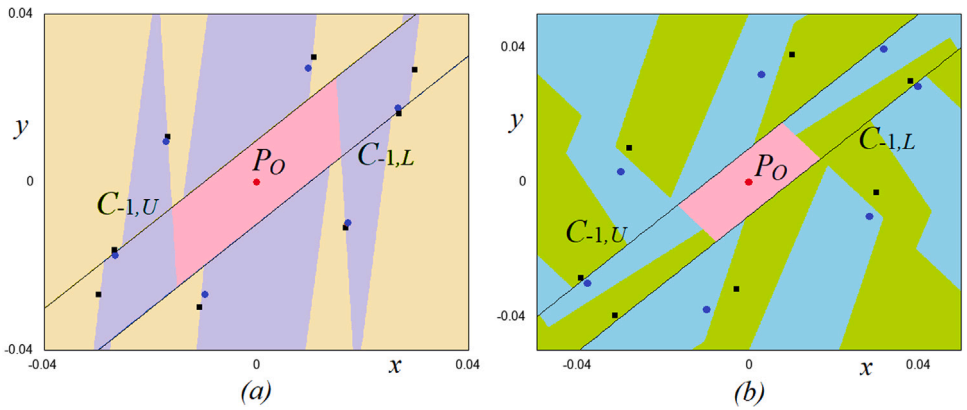

Fig. 4. Basins of attraction of the fixed point P_O coexisting with (a) one 6-cycle L^2OU^2O and one 8-cycle L^3OU^3O; (b) two 7-cycles, L^3OU^2O and U^3OL^2O. Here, $h = 0.01$, $d = 0.02$, and (a) $b = 0.03$, $c = 0.644$; (b) $b = 0.35$, $c = 0.8$.

The aforementioned cycles can be grouped into two kinds of families: the *first kind* includes cycles without points in D_O, that is, even-period cycles L^mU^m, $m \geq 1$ and odd-period cycles L^mU^{m-1}, U^mL^{m-1}, $m \geq 2$, while the *second kind* includes cycles with points in D_O, that is, even-period cycles L^mOU^mO, $m \geq 1$, and odd-period cycles L^mOU^m, U^mOL^m, $m \geq 1$. In the present paper, we focus on these two simplest kinds of families. However, it is important to emphasize that map T can have other kinds of cycles, such as odd-period cycles with symbolic sequences $L^mOU^{m-1}O$, $U^mOL^{m-1}O$, $n = 2m+1$, $m \geq 2$, each cycle having two points in D_O. One example is shown in Fig. 4b, where 7-cycles L^3OU^2O, U^3OL^2O coexist with the fixed point P_O.

Before we continue, let us state a property related to the stability of any cycle of map T. Taking into account that the Jacobian matrix J is the same in all the partitions, it follows that the eigenvalues $\lambda_1^{(n)}$ and $\lambda_2^{(n)}$ of an n-cycle are $\lambda_1^{(n)} = \lambda_1^n$, and $\lambda_2^{(n)} = \lambda_2^n$, where λ_1 and λ_2 are given in (11). For $(b, c) \in S$, any cycle is attracting, while on the boundary of S defined by $c = 2(b + 1)$, the eigenvalues of an n-cycle satisfy $-1 < \lambda_1^{(n)} < 0$, $\lambda_2^{(n)} = -1$ for odd n, and $0 < \lambda_1^{(n)} < 1$, $\lambda_2^{(n)} = 1$ for even n. Thus, we can state the following

Property 2 (*Bifurcations on the Borders of the Stability Box*). *(i) Let* $0 < b < 1$. *The condition* $c = 2(b+1)$ *corresponds to a degenerate bifurcation with eigenvalue* -1 *for any odd-period n-cycle,* $n \geq 3$, *of map T, as well as to a degenerate bifurcation with eigenvalue* $+1$ *for any even-period n-cycle,* $n \geq 2$, *of map T.*

(ii) Let $b = 1$, $0 < c < 4$. *Then the fixed point* P_O *is a center, with complex conjugate eigenvalues equal to* 1 *in modulus; in the phase plane, an invariant region with bounded dynamics exists.*

Given that the eigenvalues $\lambda_1^{(n)}$ and $\lambda_2^{(n)}$ of an n-cycle do not depend on h, Property 2*(i)* is the same as in the case $h = 0$. Property 2*(ii)* is due to region D_O in which the fixed point P_O exists, and since the map is linear in D_O, at the center bifurcation related to the fixed point with complex conjugate eigenvalues on the unit circle, some invariant sets must necessarily exist. We shall come back to this property in Section 4.7, evidencing the existence of the region with bounded dynamics, which is a new property with respect to the case $h > 0$.

It is worth emphasizing a further difference between the cases $h = 0$ and $h > 0$. Recall that for $h = 0$, an attracting n-cycle, $n \geq 3$, loses stability at $c = 2(b + 1)$ and persists for $c > 2(b + 1)$ becoming a saddle, while for $h > 0$, this is no longer always true because in this case the existence of a cycle is conditioned by other possible BCBs (due to the presence of two borders instead of one in the definition of the partitions). For example, the 4-cycle L^2U^2 for $h > 0$, similar to the case for $h = 0$, loses stability at $c = 2(b + 1)$ (the upper boundary of the stability box S) becoming a saddle. For $h = 0$, however, it persists for any $c > 2(b + 1)$, while for $h > 0$ it disappears due to a BCB when its two points collide with the borders of D_O, i.e., with the critical lines $C_{-1,L}$ and $C_{-1,U}$.

Note also that from Property 2*(i)* it follows that when in the (b, c)-plane a parameter point crosses the line $c = 2(b + 1)$, $0 < b < 1$, from below to above, in the phase plane a transition occurs from regular dynamics (no repelling cycle – expanding or saddle – can exist for $c < 2(b + 1)$) to chaotic dynamics (no attracting cycle can exist for $c > 2(b+1)$). When there is a bounded attracting set, it is necessarily chaotic, but divergent trajectories also are present. It may hold that almost all the trajectories are divergent (this occurs for parameters in the gray region of Fig. 1b). Similar to the case with $h = 0$, for $h > 0$ the transition to generic divergence is related to the first homoclinic bifurcation of the saddle 2-cycle, but now this bifurcation can occur in two different ways, leading to the two different bifurcation curves shown in Fig. 1b, denoted by H_2^U and H_2^L, and determined in Section 4.2.

4.2. Chaotic attractors and bifurcations of the 2-cycle LU

The 2-periodic points $p_0 = (x_0, y_0) \in D_L$ and $p_1 = (x_1, y_1) \in D_U$ of the 2-cycle LU are given by

$$x_0 = \frac{d}{c - 2(1 + b)}, \; y_0 = \frac{-d}{c - 2(1 + b)}, \; x_1 = -x_0, \; y_1 = -y_0. \tag{15}$$

At $c = 2(b+1)$, $0 < b < 1$, this cycle appears via degenerate transcritical bifurcation, and for $c \gtrapprox 2(b+1)$ its periodic points are close to infinity. Increasing c, both points p_0 and p_1 tend to the origin, so that at some parameter value a BCB must occur when p_0 collides with the critical lines $C_{-1,L}$ and p_1 with $C_{-1,U}$, and after this collision the 2-cycle LU disappears. Substituting (15) to the BCB condition $(x_0, y_0) \in C_{-1,L}$ (or $(x_1, y_1) \in C_{-1,U}$), we get

$$\frac{-d}{c - 2(1 + b)} = \frac{d}{c - 2(1 + b)} - h,$$

so that the BCB curve valid for $h > 0$ is defined by

$$c = 2(1 + b) + \frac{2d}{h}. \tag{16}$$

The role of the stable invariant set of the saddle 2-cycle LU for $2(1 + b) < c < 2(1 + b) + \frac{2d}{h}$, $0 < b < 1$, $h > 0$, is the same as for $h = 0$.

Since no attracting cycle can exist for $c > 2(1 + b)$ and all existing cycles are saddles (possibly homoclinic), when bounded dynamics exist, these cycles must belong to some chaotic set. The unstable invariant set of the 2-cycle has one branch whose points have divergent trajectories, while points of the opposite branch have trajectories converging to some bounded attracting set, when it exists. That is, the chaotic attractor is the ω-limit set of such a branch of the unstable invariant set of the 2-cycle. Thus, the stable invariant set of the 2-cycle, together with proper segments of the critical lines $C_{-1,L}$, $C_{-1,U}$ and their preimages, separate the region of diverging trajectories from the basin of

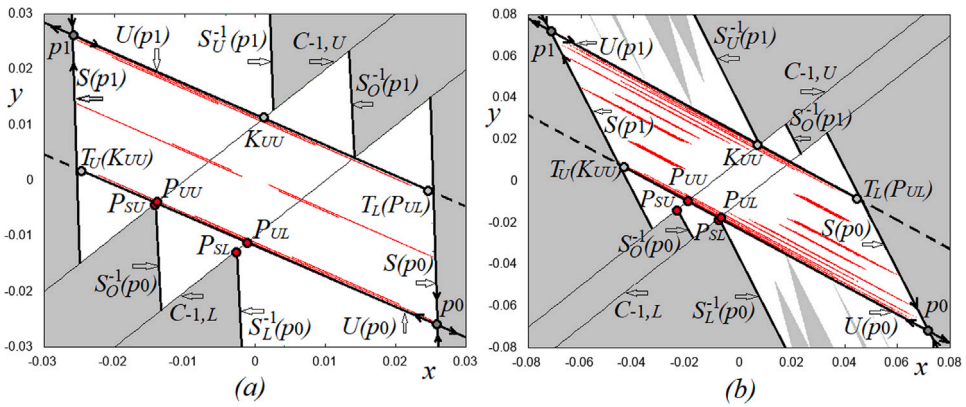

Fig. 5. Phase portrait of map T near the first homoclinic bifurcation of the 2-cycle LU when (a) $P_{SU} \approx P_{UU}$ at $b = 0.05$, $c = 2.87$; (b) $P_{SL} \approx P_{UL}$ at $b = 0.6$, $c = 3.48$. Other parameters $d = 0.02$, $h = 0.01$.

attraction of the chaotic attractors existing as long as the 2-cycle is nonhomoclinic. In this way, the boundary of the divergence region in the (b, c)-parameter plane is associated with the first homoclinic bifurcation of the 2-cycle LU, which may occur in two different ways. In fact, for $h > 0$, this boundary is formed by two curves denoted by H_2^U and H_2^L in Fig. 1b, associated with the two possible conditions of homoclinic bifurcations as explained below.

Let us first define the branches of the stable and unstable invariant sets of the saddle 2-cycle LU, which will then help us to obtain the homoclinic bifurcation conditions. As illustrated in Fig. 5, two branches of the local invariant stable set of LU, denoted by $S(p_0)$ and $S(p_1)$, are halflines of equations $y = (x - x_0)/\lambda_1 + y_0$ and $y = (x - x_1)/\lambda_1 + y_1$, issuing from a point of $C_{-1,L}$ and a point of $C_{-1,U}$, respectively. The two branches of the local unstable invariant set of LU are halflines of equations

$$y = (x - x_0)/\lambda_2 + y_0, \tag{17}$$

and

$$y = (x - x_1)/\lambda_2 + y_1, \tag{18}$$

issuing from a point $P_{UL} \in C_{-1,L}$ and a point $K_{UU} \in C_{-1,U}$. We denote by $U(p_0)$ the segment $(p_0, T_U(K_{UU}))$ of the unstable invariant set of LU, which is an image by T_U of the segment (p_1, K_{UU}), and $U(p_1)$ denotes the segment $(p_1, T_L(P_{UL}))$, which is an image by T_L of the segment (p_0, P_{UL}). Obviously, segments $U(p_0)$ and $U(p_1)$ belong to the straight lines of the same equations given above, of the local unstable invariant sets of LU, namely, $y = (x - x_0)/\lambda_2 + y_0$ and $y = (x - x_1)/\lambda_2 + y_1$, respectively.

In Fig. 5, we illustrate two different cases of the phase portrait of map T near the first homoclinic bifurcation of the 2-cycle LU. To obtain the related conditions, we need two more branches of the stable invariant set of LU. We first take a preimage by map T_L^{-1} of branch $S(p_0)$, which is denoted by $S_L^{-1}(p_0)$. Obviously, the preimage by map T_U^{-1} of $S(p_0)$ is branch $S(p_1)$. Applying T_L^{-1} to $S(p_0)$, branch $S_L^{-1}(p_0)$ is obtained, which belongs to the line of equation

$$y = ((v - \lambda_1)x + \lambda_1 y_0 - x_0 + d)/b, \tag{19}$$

and applying T_O^{-1} to $S(p_0)$, branch $S_O^{-1}(p_0)$ is obtained, which belongs to the line of equation

$$y = ((v - \lambda_1)x + \lambda_1 y_0 - x_0)/b. \tag{20}$$

In Fig. 5a, we see that the first contact of the stable and unstable invariant sets of LU can be determined from the condition $P_{UU} = P_{SU}$, while in Fig. 5b the first contact corresponds to the condition $P_{UL} = P_{SL}$, where points P_{UU} and P_{SU} are intersection points of the branches $U(p_0)$ and $S_O^{-1}(p_0)$ with the critical line $C_{-1,U}$, while P_{UL} and P_{SL} are intersection points of the branches $U(p_0)$ and $S_L^{-1}(p_0)$ with the critical line $C_{-1,L}$. Using Eqs. (17), (13), (20), and (19), these intersection points can be easily obtained: point P_{UU} is given by $x = x'' = \frac{y_0 - x_0/\lambda_2 - h}{1 - 1/\lambda_2}$, $y = y'' = x'' + h$; point P_{SU} is given by $x = \overline{x} = \frac{\lambda_1 y_0 - x_0 - bh}{c - 1 + \lambda_1}$, $y = \overline{y} = \overline{x} + h$; point P_{UL} is given by $x = x' = \frac{y_0 - x_0/\lambda_2 + h}{1 - 1/\lambda_2}$, $y = y' = x' - h$; and point P_{SL} is given by $x = \widetilde{x} = \frac{\lambda_1 y_0 - x_0 + d + bh}{c - 1 + \lambda_1}$, $y = \widetilde{y} = \widetilde{x} - h$.

In this way, the first homoclinic bifurcation of LU can be defined from the condition $\overline{x} = x''$, related to $P_{UU} = P_{SU}$ (in Fig. 5a, points P_{UU} and P_{SU} almost coincide), leading to the first homoclinic bifurcation curve denoted H_2^U :

$$(H_2^U) \quad \frac{y_0 - x_0/\lambda_2 - h}{1 - 1/\lambda_2} = \frac{\lambda_1 y_0 - x_0 - bh}{c - 1 + \lambda_1}, \tag{21}$$

or from the condition $\widetilde{x} = x'$ related to $P_{UL} = P_{SL}$ (in Fig. 5b, the points P_{UL} and P_{SL} almost coincide) leading to the first homoclinic bifurcation curve denoted H_2^L :

$$(H_2^L) \quad \frac{y_0 - x_0/\lambda_2 + h}{1 - 1/\lambda_2} = \frac{\lambda_1 y_0 - x_0 + d + bh}{c - 1 + \lambda_1}. \tag{22}$$

As can be seen in Fig. 1b, for the parameter values under consideration, these curves intersect at a point, say H_2, of the feasible parameter domain. As a result, on the left/right of the intersection point H_2, curve H_2^U/H_2^L is valid, and it corresponds to the first homoclinic bifurcation of the 2-cycle LU.

Since the homoclinic bifurcation corresponds to a contact of the chaotic set with the stable and unstable invariant sets of the saddle 2-cycle, and the stable invariant set is on the boundary of the set of divergent trajectories, after the first homoclinic bifurcation almost all the trajectories are divergent, although a chaotic repeller still exists, which includes infinitely many homoclinic saddle cycles and their stable sets.

We have therefore proved the following

Property 3 (*Chaotic Attractor, 2-Cycle and Related Bifurcations*). *Let* $0 < b < 1$, $h > 0$, *then*

(i) the saddle 2-cycle LU with periodic points given in (15) exists for $2(b + 1) < c < 2(1 + b) + \frac{2d}{h}$;

(ii) for parameters (b, c) *belonging to the region above line* $c = 2(b + 1)$ *and below the homoclinic bifurcation curves* H_2^U / H_2^L *given in (21) and (22), the stable invariant set of the 2-cycle belongs to the boundary of the region of bounded trajectories, where a chaotic attracting set of map T exists. For parameters above the homoclinic bifurcation curves* H_2^U / H_2^L, *the generic trajectory is divergent.*

To end this section, it is worth noting that the structure of the existing chaotic attractor is similar to the one occurring in a 2D piecewise-linear discontinuous map defined on two partitions, known as the Belykh map (see [27,32]), which is characterized by a region in the phase space in which all cycles are saddles. Moreover, similar

to our case, the basin boundary of a chaotic attractor in the Belykh map is associated with the stable invariant set of a saddle 2-cycle, and the chaotic attractor exists up to the first homoclinic bifurcation of this cycle. This is clearly true in the case $h = 0$, when the map in defined on two partitions (as for the Belykh map), but we have the numerical evidence that this is true also in the case $h > 0$, when the map is defined on three partitions. This is a novelty for the understanding of the properties of the chaotic set in terms of ergodic theory (related to the property that all existing cycles are saddles).

4.3. Even-period cycles in two partitions, L^mU^m, $m \geq 1$

Let us now determine the boundaries of the largest periodicity regions related to attracting cycles with rotation number $1/n$. We begin with a cycle L^mU^m, $m \geq 1$. Its periodic points have been detected for the case $h = 0$ (see [12]), and this result is also valid for the case $h > 0$. However, the corresponding periodicity region is bounded by curves related to different BCBs. Let $p_0 = (x_0, y_0)$ be the point of a $2m$-cycle L^mU^m, $m \geq 1$, which is the leftmost periodic point in partition D_L, that is, with $y_0 < x_0 - h$. Then from $T_L^m(x_0, y_0) = (-x_0, -y_0)$ it holds that

$$\begin{pmatrix} x_0 \\ y_0 \end{pmatrix} = \frac{d/c}{P_{J^m}(-1)} \begin{pmatrix} b^m - 1 + a_{m-1}(1 - b - c) \\ b^m - 1 + a_{m-1}(1 - b + c) \end{pmatrix}, \tag{23}$$

where

$$P_{J^m}(-1) = 1 + 2a_m - va_{m-1} + b^m$$

is the characteristic polynomial $P_{J^m}(\lambda)$ of matrix J^m evaluated at $\lambda = -1$, and

$$a_m = va_{m-1} - ba_{m-2},\ m \geq 2$$

is a second-order linear difference equation with the initial conditions

$$a_0 = 1,\ a_1 = v.$$

One can check that substituting $m = 1$ to (23), we obtain point p_0 of the 2-cycle considered above (see (15)).

The existence conditions of cycle L^mU^m, that is, the conditions which guarantee that all points belong to their proper partitions, are given by the following inequalities, which must be satisfied simultaneously:

$$\begin{cases} (c1) & y_0 \leq x_0 - h & (p_0 \in D_L), \\ (c2) & y_{m-1} \leq x_{m-1} - h & (p_{m-1} \in D_L). \end{cases} \tag{24}$$

Note that due to the symmetry of map T, conditions (c1) and (c2) in (24) can be equivalently written as $y_m \geq x_m + h$ and $y_{n-1} \geq x_{n-1} + h$ ($p_{n-1} \in D_U$), respectively. That is, if conditions (c1) and (c2) in (24) are satisfied, then all the points of cycle L^mU^m are in their proper partitions.

Substituting x_0 and y_0 from (23) to the existence condition (c1) in (24), we get

$$\frac{2da_{m-1}}{P_{J^m}(-1)} \leq -h, \tag{25}$$

where equality corresponds to the condition $p_0 \in C_{-1,L}$, that is, to the condition of the first BCB of cycle L^mU^m. Due to the symmetry of L^mU^m with respect to the origin, it holds that $p_m \in C_{-1,U}$. The related BCB curves are denoted by $B_{2m}^{1,1}$ and plotted in Fig. 6a for $m = 2, \ldots, 8$. They are the lower boundaries of the $2m$-periodicity regions. The upper index "1,1" in $B_{2m}^{1,1}$ denotes that it is the first BCB condition of the first kind of family of cycles (without points in D_O).

The simplest way to obtain the existence condition (c2) in (24) is to take a preimage of p_0 by

$$T_U^{-1} : \begin{pmatrix} x \\ y \end{pmatrix} \to \begin{pmatrix} y \\ (-x + vy - d)/b \end{pmatrix},$$

so that

$$\begin{pmatrix} x_{n-1} \\ y_{n-1} \end{pmatrix} = \begin{pmatrix} y_0 \\ (-x_0 + vy_0 - d)/b \end{pmatrix}.$$

Substituting x_0 and y_0 from (23), we get

$$\begin{pmatrix} x_{n-1} \\ y_{n-1} \end{pmatrix} = \frac{d/c}{P_{J^m}(-1)} \begin{pmatrix} b^m - 1 + a_{m-1}(1 - b + c) \\ b^m - 1 + a_{m-1}(1 - b + c) - 2c(b^{m-1} - a_{m-2}) \end{pmatrix}, \tag{26}$$

and substituting the expressions for x_{n-1} and y_{n-1} from (26) into $y_{n-1} \geq x_{n-1} + h$ (this inequality is equivalent to the existence condition (c2) in (24)), we get

$$\frac{2d(a_{m-2} - b^{m-1})}{P_{J^m}(-1)} \geq h. \tag{27}$$

Here, equality corresponds to the condition $p_{n-1} \in C_{-1,U}$ (as well as $p_{m-1} \in C_{-1,L}$), that is, to the condition of the second BCB of cycle L^mU^m. The related BCB curves are denoted by $B_{2m}^{2,1}$ and plotted in Fig. 6a for $m = 2, \ldots, 8$. They are the upper boundaries of the $2m$-periodicity regions.

As an example, let us consider the 4-cycle L^2U^2. Its point $p_0 \in D_L$ is obtained from (23) for $m = 2$:

$$x_0 = \frac{d(c - 2)}{1 + 2a_2 - va_1 + b^2},\quad y_0 = \frac{d(2b - c)}{1 + 2a_2 - va_1 + b^2}.$$

Substituting $m = 2$ to (25), we get that the condition $y_0 \leq x_0 - h$ is satisfied for

$$c \geq (1 + b) + \frac{h}{2d}(1 + 2a_2 - va_1 + b^2), \tag{28}$$

where $a_2 = v^2 - b$, $a_1 = v$, so that $(1 + 2a_2 - va_1 + b^2) = (1 - b)^2 + v^2 > 0$. This equality corresponds to the lower BCB boundary $B_4^{1,1}$ of the 4-periodicity region related to cycle L^2U^2 (see Fig. 6a).

The second BCB condition is obtained by substituting $m = 2$ to (27):

$$h(1 + 2a_2 - va_1 + b^2) \leq 2d(1 - b), \tag{29}$$

which (for $0 < b < 1$) is always satisfied in the case $h = 0$, while this is no longer true for $h > 0$, leading to the second BCB condition, which defines the upper BCB boundary $B_4^{2,1}$ of the 4-periodicity region related to the cycle L^2U^2 (see Fig. 6a). In Fig. 6b, cycle L^2U^2 is close to this BCB. As can be seen in Fig. 6a, curve $B_4^{2,1}$ can be crossed when cycle L^2U^2 is still attracting (i.e., for $c < 2(b + 1)$), as well as when it is a saddle (for $c > 2(b + 1)$).

4.4. Odd-period cycles in two partitions, L^mU^{m-1}, U^mL^{m-1}, $m \geq 2$

Let us suppose that map T has a cycle of odd period $n = 2m - 1$, $m \geq 2$, with symbolic sequence L^mU^{m-1}. Then a symmetric cycle U^mL^{m-1} must also exist. Let the point $p_0 = (x_0, y_0)$ of a cycle L^mU^{m-1} be the leftmost point in the lower partition. From $T_U^{m-1} \circ T_L^m(x_0, y_0) = (x_0, y_0)$, we get

$$\begin{pmatrix} x_0 \\ y_0 \end{pmatrix} = \frac{d/c}{P_{J^{2m-1}}(1)} \begin{pmatrix} P_{J^{2m-1}}(1) - 2(ba_{2m-3} + 1)k_1 + 2ba_{2m-2}k_2 \\ P_{J^{2m-1}}(1) - 2a_{2m-2}k_1 + 2(a_{2m-1} - 1)k_2 \end{pmatrix}, \tag{30}$$

where, for short,

$$k_1 = 1 - a_{m-1} + ba_{m-2},\ k_2 = 1 - a_{m-2} + ba_{m-3},$$

and

$$P_{J^{2m-1}}(1) = 1 - a_{2m-1} + ba_{2m-3} + b^{2m-1}.$$

Note that the point $(-x_0, -y_0)$ is the rightmost point of the symmetric cycle U^mL^{m-1} in the upper partition.

For example, for the 3-cycle L^2U ($m = 2$ in (30)), we get

$$x_0 = \frac{d\left(b^2 + b + 1 - c\,(b - c + 3)\right)}{c[3(b^2 + b + 1) - c(3b - c + 3)]},\quad y_0 = \frac{d(b^2 + b + 1 + c(b - c + 1))}{c[3(b^2 + b + 1) - c(3b - c + 3)]}.$$

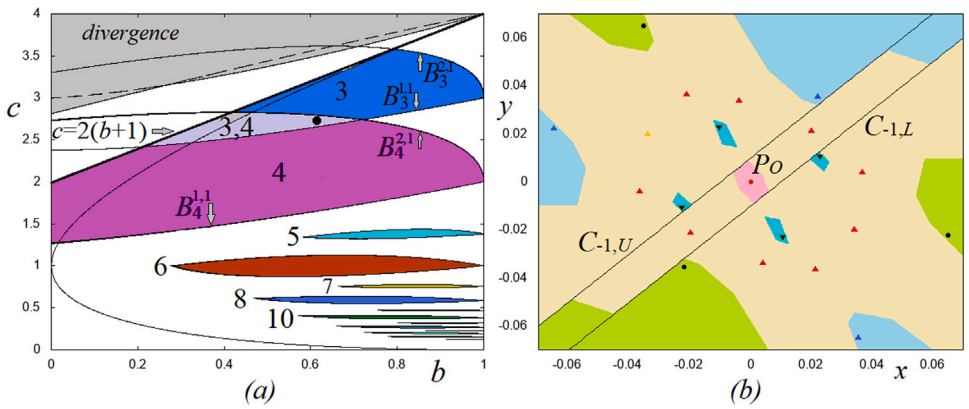

Fig. 6. (a) BCB boundaries of the periodicity regions related to even-period cycles L^mU^m and pairs of odd-period cycles L^mU^{m-1}, U^mL^{m-1} for $m = 2, \dots, 8$; (b) basins of coexisting attracting fixed point P_O, 4-cycle L^2U^2, 3-cycles L^2U, U^2L, and 10-cycle L^2UOLU^2LOU at $b = 0.61$, $c = 2.67$ (the related parameter point is indicated by a black circle in (a)). Other parameters are $d = 0.02$, $h = 0.01$.

For the existence of L^2U, inequality $y_0 < x_0 - h$ must be satisfied. It can be checked that inequality $[3(b + b^2 + 1) - c(3b - c + 3)] > 0$ always holds, and the existence condition $y_0 \le x_0 - h$ leads to

$$2d(b + 2 - c) \le -h[3(b + b^2 + 1) - c(3b - c + 3)].$$

In particular, for $h = 0$, we have the condition $c \ge b+2$. Equality defines the lower BCB curve $B_3^{1,1}$ (see Fig. 6a). Considering the point $(-x_0, -y_0)$ of the symmetric cycle U^2L, its existence condition $-y_0 > -x_0 + h$ obviously leads to the same inequality. In Fig. 6b, the 3-cycles L^2U and U^2L are near this BCB.

For a generic cycle L^mU^{m-1} (as well as for the symmetric cycle U^mL^{m-1}), the existence conditions are given by (c1) and (c2) in (24). Substituting x_0 and y_0 from (30) to condition (c1) in (24), we get

$$\frac{2d(k_1(-a_{2m-2} + ba_{2m-3} + 1) + k_2(a_{2m-1} - ba_{2m-2} - 1))}{P_{J^{2m-1}}(1)c} \le -h. \tag{31}$$

Equality defines the lower BCB boundary $B_{2m-1}^{1,1}$ of the $(2m - 1)$ - periodicity regions of the first kind of family of cycles (i.e., cycles without points in D_O), which are plotted for $m = 2, \dots, 8$ in Fig. 6a.

For condition (c2) in (24), we need point $p_{m-1} = T_L^{m-1}(p_0)$, which after straightforward computations, can be defined as

$$\begin{pmatrix} x_{m-1} \\ y_{m-1} \end{pmatrix} = J^{m-1}\frac{d/c}{P_{J^{2m-1}}(1)}\begin{pmatrix} P_{J^{2m-1}}(1) - 2(ba_{2m-3} + 1)k_1 + 2ba_{2m-2}k_2 \\ P_{J^{2m-1}}(1) - 2a_{2m-2}k_1 + 2(a_{2m-1} - 1)k_2 \end{pmatrix} + \frac{d}{c}\begin{pmatrix} k_1 \\ k_2 \end{pmatrix}, \tag{32}$$

where the macro parameters k_1, k_2, and $P_{J^{2m-1}}(1)$ are the same as above.

In particular, for the 3-cycle L^2U $(m = 2)$, its point (x_1, y_1) is as follows:

$$x_1 = \frac{d(b^2 + b + 1 - c(1 + 3b - c))}{c\left(3(b + b^2 + 1) - c(3b - c + 3)\right)}, \quad y_1 = \frac{d\left(b^2 + b + 1 - c\,(b - c + 3)\right)}{c\left(3(b + b^2 + 1) - c(3b - c + 3)\right)}.$$

Inequality $y_1 \le x_1 - h$ leads to the condition $-2d(1 - b) \le -h[3(b + b^2 + 1) - c(3b - c + 3)]$, that is

$$2d(1 - b) \ge h[3(b + b^2 + 1) - c(3b - c + 3)].$$

For $b < 1$, the existence condition is always satisfied in the case $h = 0$, while for $h > 0$, equality defines the upper BCB boundary $B_3^{2,1}$ of the related periodicity region (see Fig. 6a). When these boundaries are crossed, cycles L^2U and U^2L disappear. As can be seen in Fig. 6a, boundary $B_3^{2,1}$ can be crossed when the cycles under consideration are attracting (for $c < 2(b + 1)$) or saddle (for $c > 2(b + 1)$). Moreover, this BCB can also occur when almost all the trajectories are diverging (above the homoclinic bifurcation curve of the 2-cycle LU).

For a generic cycle L^mU^{m-1} (as well as for the symmetric cycle U^mL^{m-1}), substituting x_{m-1}, y_{m-1} from (32) to $y_{m-1} \le x_{m-1} - h$, the existence condition (c2) in (24) can be simplified as follows:

$$\frac{ba_{2m-2}(a_{m-3}(1 + ba_{m-3}) - a_{m-2}^2) - a_{m-2}(ba_{2m-3} + 1)(1 - a_{m-1} + ba_{m-3})}{P_{J^{2m-1}}(1)} \le -hc/2d.$$

Equality defines the upper BCB boundaries $B_{2m-1}^{2,1}$ of the $(2m - 1)$-periodicity regions of the first family of cycles, which are plotted for $m = 2, \dots, 8$ in Fig. 6a.

4.5. Even-period cycles in three partitions, L^mOU^mO, $m \ge 1$

We now turn to the second kind of families of cycles, with points in all three partitions. The simplest symbolic sequences are those of even-period cycles L^mOU^mO, $m \ge 1$. Let us denote again as $p_0 = (x_0, y_0)$ the leftmost point in D_L of a cycle L^mOU^mO. By using the symmetry with respect to the origin, it can be obtained from $T_O \circ T_L^m(x_0, y_0) = (-x_0, -y_0)$, leading to

$$\begin{pmatrix} x_0 \\ y_0 \end{pmatrix} = \frac{d/c}{P_{J^{m+1}}(-1)}\begin{pmatrix} c(1 - a_m - ba_{m-1}) + a_m(1 - b) + b^{m+1} - 1 \\ a_m(1 - b) + b^{m+1} - 1 \end{pmatrix}, \tag{33}$$

where

$$P_{J^{m+1}}(-1) = 1 + a_{m+1} - ba_{m-1} + b^{m+1}.$$

The existence conditions of the cycle L^mOU^mO are given by the following inequalities, which must be satisfied simultaneously:

$$\begin{cases} \text{(c1)} & y_0 \le x_0 - h & (p_0 \in D_L), \\ \text{(b1)–(b2)} & x_m - h \le y_m \le x_m + h & (p_m \in D_O), \\ \text{(c2)} & y_{m-1} \le x_{m-1} - h & (p_{m-1} \in D_L), \end{cases} \tag{34}$$

where conditions (c1) and (c2) are as in (24), and now condition (c2) can be equivalently written as $y_{n-2} \ge x_{n-2} + h$ $(p_{n-2} \in D_U)$. Similarly, conditions (b1) and (b2) in (34) can be equivalently written as $x_{n-1} - h \le y_{n-1} \le x_{n-1} + h$ $(p_{n-1} \in D_O)$.

Substituting (33) to condition (c1) leads to the following inequality:

$$\frac{d(a_m + ba_{m-1} - 1)}{P_{J^{m+1}}(-1)} \le -h,$$

where equality corresponds to the BCB occurring when $p_0 \in C_{-1,L}$. The corresponding curve is denoted by $B_n^{1,2}$ (here, the upper index 2 indicates the second kind of family of cycles, to distinguish from the previous kind of family with no points in D_O).

To obtain conditions (b1)–(b2) in (34) in the form $x_{n-1} - h \le y_{n-1} \le x_{n-1} + h$, we need point p_{n-1}, which can be obtained by taking the

preimage by T_O^{-1} of point p_0 :

$$\begin{pmatrix} x_{n-1} \\ y_{n-1} \end{pmatrix} = \begin{pmatrix} y_0 \\ (-x_0 + \upsilon y_0)/b \end{pmatrix},$$

which leads to

$$\begin{pmatrix} x_{n-1} \\ y_{n-1} \end{pmatrix} = \frac{d/c}{P_{J^{m+1}}(-1)} \begin{pmatrix} a_m(1-b) + b^{m+1} - 1 \\ a_m(1-b) + b^{m+1} - 1 + c(a_{m-1} + a_m - b^m) \end{pmatrix}. \tag{35}$$

Then conditions (b1)–(b2) simplifies to

$$-h \le \frac{d(a_{m-1} + a_m - b^m)}{P_{J^{m+1}}(-1)} \le h,$$

where the left equality corresponds to the BCB at which $p_{n-1} \in C_{-1,L}$, and the right equality to the BCB at which $p_{n-1} \in C_{-1,U}$. The related BCB curves are denoted by $B_n^{2,2}$ and $B_n^{3,2}$, respectively.

Finally, to obtain condition (c2) in the form $y_{n-2} \ge x_{n-2} + h$ ($p_{n-2} \in D_U$), we need point p_{n-2}, which we obtain by taking the preimage by T_U^{-1} of point p_{n-1} :

$$\begin{pmatrix} x_{n-2} \\ y_{n-2} \end{pmatrix} = \begin{pmatrix} y_{n-1} \\ (-x_{n-1} + \upsilon y_{n-1} - d)/b \end{pmatrix},$$

$$\begin{pmatrix} x_{n-2} \\ y_{n-2} \end{pmatrix} = \frac{d/c}{P_{J^{m+1}}(-1)} \begin{pmatrix} a_m(1-b) + b^{m+1} - 1 + c(a_{m-1} + a_m - b^m) \\ ((b-c)k + \upsilon c(a_{m-1} + a_m - b^m) - c(1 + a_{m+1} - b a_{m-1} + b^{m+1}))/b \end{pmatrix}.$$

Condition (c2) can then be written as $(-x_{n-1} + \upsilon y_{n-1} - d)/b \ge y_{n-1} + h$, and substituting x_{n-1}, y_{n-1} from (35), this condition simplifies to

$$\frac{(1 + 2b - c)(a_{m-1} - b^m) - a_m}{P_{J^{m+1}}(-1)} \ge \frac{bh}{d},$$

where equality corresponds to the BCB at which $p_{n-2} \in C_{-1,U}$. The related BCB curve is denoted by $B_n^{4,2}$.

In Fig. 7a, the BCB curves bounding the existence regions of even-period cycles $L^m OU^m O$ are plotted for $m = 1, \dots, 5$. In particular, the indicated BCB curves $B_4^{1,2}$, $B_4^{2,2}$, $B_4^{3,2}$, and $B_4^{4,2}$ bound the existence region of the 4-cycle $LOUO$. Note that in this specific case, curves $B_4^{1,2}$ and $B_4^{4,2}$ coincide. In fact, for cycle $LOUO$, the condition $p_0 \in C_{-1,L}$ of $B_4^{1,2}$ and $p_{m-1} \in C_{-1,L}$ of $B_4^{4,2}$ are the same, since in the considered case $m = 1$. Other even-period regions in Fig. 6a are bounded by curves $B_n^{2,2}$, $B_n^{3,2}$, and $B_n^{4,2}$ only, that is, for the parameter values under consideration, curve $B_n^{1,2}$ is not involved.

4.6. Odd-period cycles in three partitions, $L^m OU^m$, $U^m OL^m$, $m \ge 1$

Let us now consider the simplest odd-period cycles with points in all three partitions, namely, cycles $L^m OU^m$ and their symmetric cycles with respect to the origin, with symbolic sequence $U^m OL^m$, $m \ge 1$. As before, let $p_0 = (x_0, y_0)$ be the point of cycle $L^m OU^m$, which is the leftmost point in region D_L. This point can be obtained from $T_U^m \circ T_O \circ T_L^m (x_0, y_0) = (x_0, y_0)$, leading to

$$\begin{pmatrix} x_0 \\ y_0 \end{pmatrix} = \frac{d/c}{P_{J^{2m+1}}(1)} \begin{pmatrix} b a_{2m}\left(k3 - c a_{m-1}\right) - \left(b a_{2m-1} + 1\right)\left(k3 + c(a_m - a_{2m})\right) \\ -a_{2m}\left(k3 + c(a_m - a_{2m})\right) + \left(a_{2m+1} - 1\right)\left(k3 - c a_{m-1}\right) \end{pmatrix}, \tag{36}$$

where

$$k3 = 2ba_{m-1} - 2a_m + a_{2m} - ba_{2m-1} + 1,$$
$$P_{J^{2m+1}}(1) = 1 - a_{2m+1} + ba_{2m-1} + b^{2m+1}.$$

The existence conditions of cycle $L^m OU^m$ are given by the conditions (c1), (b1)–(b2) in (34), that must be satisfied simultaneously. Condition (c1) holds for

$$\frac{-a_{2m}(a_{m-1}(2b - c) - 2a_m + 2) + (ba_{2m-1} - a_{2m} + 1)(a_m + a_{m-1})}{P_{J^{2m+1}}(1)} \le h/d,$$

where equality corresponds to the BCB of $L^m OU^m$ occurring when $p_0 \in C_{-1,L}$ (and it holds also that the symmetric point of cycle $U^m OL^m$ belongs to $C_{-1,U}$). We denote the related bifurcation curve as $B_n^{1,2}$.

To obtain conditions (b1)-(b2), we need point p_m of cycle $L^m OU^m$, which can be obtained from $(x_m, y_m) = T_U^m(x_0, y_0)$:

$$\begin{pmatrix} x_m \\ y_m \end{pmatrix} = \begin{pmatrix} d/c(1 - a_m + ba_{m-1}) + a_m x_0 - ba_{m-1} y_0 \\ d/c(1 - a_{m-1} + ba_{m-2}) + a_{m-1} x_0 - ba_{m-2} y_0 \end{pmatrix}.$$

Condition (b1), that is, $y_m \ge x_m - h$, can be written as

$$-a_{m-1}d + (a_{m-1} - a_m)x_0 - (a_{m-2} - a_{m-1})by_0 \le -h,$$

and condition (b2), that is, $y_m \le x_m + h$, as

$$-a_{m-1}d + (a_{m-1} - a_m)x_0 - (a_{m-2} - a_{m-1})by_0 \ge h,$$

where x_0, y_0 are given in (36). The corresponding BCB boundaries, related to equalities, are denoted by $B_n^{2,2}$ ($p_m \in C_{-1,L}$) and $B_n^{3,2}$ ($p_m \in C_{-1,U}$), respectively.

In Fig. 7a, the BCB curves bounding the existence regions of the odd-period cycles $L^m OU^m$ are plotted for $m = 1, \dots, 4$. In particular, the indicated BCB curves $B_5^{1,2}$, $B_5^{2,2}$, and $B_5^{3,2}$ bound the existence region of the 5-cycles $L^2 OU^2$, $U^2 OL^2$. As one can see, this region overlaps with the region of the 6-cycle $L^2 OU^2 O$; in Fig. 7b, we show an example of the phase portrait with basins of these coexisting cycles, as well as the basin of attracting fixed point P_O.

For example, the existence conditions of cycles LOU and UOL ($m = 1$) are as follows:

(c1) $4b - 3c + 5 - (3b\upsilon + c(c-3) + 3)\, h/d \le 0$,
(b1) $c - 3 + (3b\upsilon + c(c-3) + 3)\, h/d \le 0$,
(b2) $c - 3 - (3b\upsilon + c(c-3) + 3)\, h/d \ge 0$,

where equalities define the BCB boundaries $B_3^{1,2}$, $B_3^{2,2}$, and $B_3^{3,2}$, respectively, of the existence region of cycles LOU and UOL. For the example shown in Fig. 7a, only boundaries $B_3^{2,2}$ and $B_3^{3,2}$ are involved. In contrast, the existence region of cycles $L^2 OU^2$ and $U^2 OL^2$ are bounded by three BCB curves, namely $B_5^{1,2}$, $B_5^{2,2}$, and $B_5^{3,2}$.

4.7. Center bifurcation and issuing points for two period-adding structures

It is useful to compare the n-periodicity regions of the first kind of family of cycles, related to periodic points only in the two partitions, L and U, and the second kind of family of cycles, with periodic points in the three partitions L, U, and O. Our aim is to show that their issuing points belong to the line defined by $b = 1$, which, in turn, is related to the center bifurcation of the fixed point P_O. In fact, we demonstrate that two periodicity regions related to two different kinds of families of attracting cycles are issuing from the same point of the center bifurcation line.

In Fig. 8a, b, c, d, such periodicity regions are superimposed for $n = 3, 4, 5, 6$, respectively. Let the points of the first kind of family of cycles (i.e., of even-period cycles $L^m U^m$, $n = 2m$, and odd-period cycles $L^m U^{m-1}$, $U^m L^{m-1}$, $n = 2m - 1$) be denoted by $\{p_i\}_{i=0}^{n-1}$, and the points of the second kind of families of cycles (i.e., of even-period cycles $L^m OU^m O$, $n = 2m + 2$, and odd-period cycles $L^m OU^m$, $U^m OL^m$. $n = 2m + 1$) be denoted by $\{q_i\}_{i=0}^{n-1}$. In Fig. 8, we have plotted the BCB conditions corresponding to each BCB curve. It can be shown that the periodicity regions of both kinds of families issue from the line defined by $\det J = b = 1$ (for $0 < c < 4$).

Moreover, we can state that for both kinds of families, a periodicity region related to attracting cycles with rotation number m/n issues from point $(b, c) = (1, c_{m/n})$, where $c_{m/n} = 2(1 - \cos 2\pi m/n)$. For example, $c_{1/3} = 3$, $c_{1/4} = 2$, $c_{1/5} = (5 - \sqrt{5})/2 \approx 1.382$, $c_{2/5} = (5 + \sqrt{5})/2 \approx 3.618$, $c_{1/6} = 1$, etc.

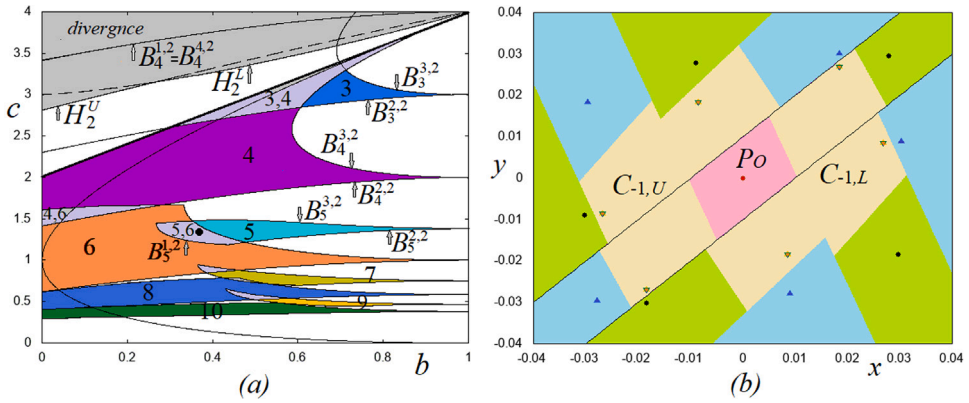

Fig. 7. (a) BCB boundaries of the periodicity regions related to even-period cycles L^mOU^mO and pairs of odd-period cycles L^mOU^{m-1}, U^mOL^m for $m = 1,\dots,4$; (b) basins of coexisting attracting fixed point P_O, 6-cycle L^2OU^2O, and 5-cycles L^2OU^2, U^2OL^2 at $b = 0.35$, $c = 1.3$ (the related parameter point is indicated by a black circle in (a)). Other parameters $d = 0.02$, $h = 0.01$.

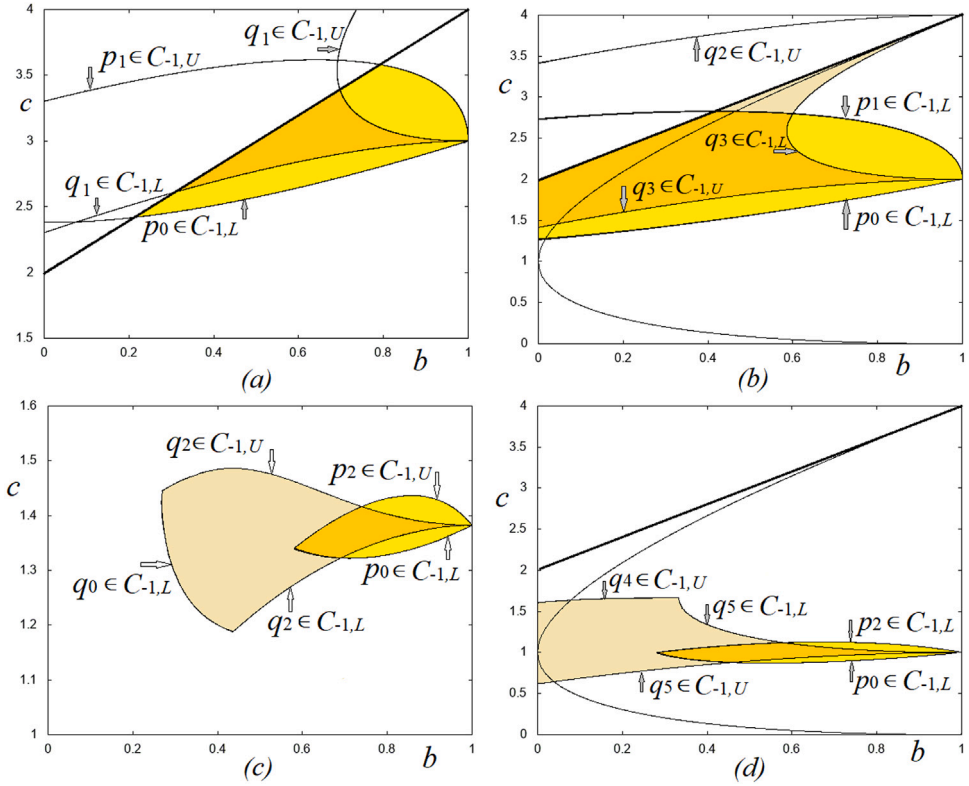

Fig. 8. n-periodicity regions of the first and second kinds of families of cycles for $n = 3$ (a), $n = 4$ (b), $n = 5$ (c), and $n = 6$ (d) in the (b, c)-parameter plane for $h = 0.01$, $d = 0.02$.

This case, at $\det J = b = 1$ in all the points of the plane, except for the two lines of discontinuity, is associated with a conservative case, and in a suitable portion of the phase plane, belonging to region D_O, the map has bounded dynamics. That is, we expect the existence of an invariant region in the strip between the two discontinuity lines at the center bifurcation value $b = 1$. Since map T_O is linear, its dynamics at $b = 1$ is well known: locally, the trajectories belong to invariant ellipses on which the trajectories are

• either all periodic (and dense on each ellipse) when the rotation number is rational, say m/n, moreover, when n is odd, due the symmetry, the existing invariant ellipses are filled with couples of cycles symmetric to each other with respect to the origin;

• or quasiperiodic (also dense on each ellipse) when the rotation number is irrational.

Here the term "locally" is related to the size of an invariant region that depends on the distance of the fixed point from the discontinuity lines. To determine the boundary of the invariant region at the center bifurcation value $b = 1$, we can follow arguments similar to those used in [25]. In fact, we have two different kinds of invariant regions, depending on the rotation number of the linear map T_O, rational or irrational:

• when the rotation number is irrational, then an invariant region exists between the two discontinuity lines, bounded by an invariant ellipse that is tangent to the two discontinuity lines; the region is filled with invariant ellipses and each ellipse is densely filled with quasiperiodic trajectories (an example is shown in Fig. 9a);

• when the rotation number is rational, say m/n, then invariant ellipses exist filled with periodic points of period n, and there exists

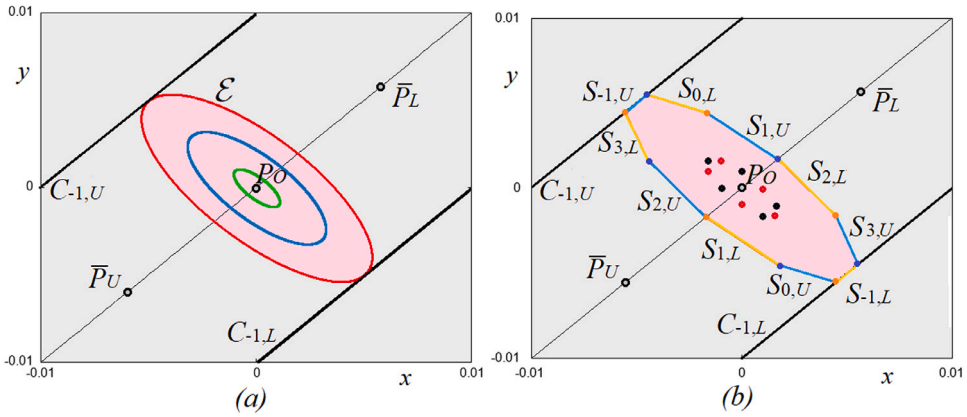

Fig. 9. Center bifurcation of the fixed point P_O. In (a) rotation number is irrational, in (b) rotation number is rational, $m/n = 2/5$. Parameter values are $b = 1$ and $c = 2(1 - \cos(\pi(1 - \sqrt{5})))$ in (a), $c = c_{2/5} = (5 + \sqrt{5})/2$ in (b).

an invariant ellipse that is tangent to the two discontinuity lines. Moreover, other periodic trajectories exist, filling a polygon whose boundary is determined by generating segments belonging to the discontinuity lines, $S_{-1,L} \subset LC_{-1,L}$ and $S_{-1,U} \subset LC_{-1,U}$, symmetric with respect to the origin. When n is even, then each segment and its images form n sides of the invariant polygon filled with cycles of even period n. When n is odd, then due the symmetry, both segments and their images are to be used, giving $2n$ sides of the invariant polygon filled with cycles of odd period n. An example is shown in Fig. 9b for $c = c_{2/5} = (5 + \sqrt{5})/2$.

This is the dynamic behavior at the bifurcation value $b = 1$; outside the invariant region, the trajectories (due to the discontinuities) are diverging. However, for low values of b, say $b = 1 - \varepsilon$, the fixed point P_O is an attracting focus, and we have seen that BCB curves are issuing from the points associated with rational rotation numbers. The peculiarity of the map on three partitions is that from each point $(b, c) = (1, c_{m/n})$, where $c_{m/n} = 2(1 - cos(2\pi m/n))$, related to a rational rotation number m/n, two different overlapping periodicity regions are issuing. The rotation numbers of the Jacobian matrix J at $b = 1$, $0 < c < 4$, can be ordered according to the Farey summation rule, so that in a left neighborhood of the line $b = 1$, the periodicity regions issuing from the related points $(b, c) = (1, c_{m/n})$ are organized in two overlapping period-adding bifurcation structures.

Note that this is a peculiarity of the case with $h > 0$, for map T defined on three partitions, since for $h = 0$, the strip between the two discontinuity lines does not exist, and from point $(b, c) = (1, c_{m/n})$ associated with rotation number m/n, only one periodicity region is issuing, bounded by BCB curves of cycles with periodic points in two partitions only.

5. Conclusions

To improve our understanding of the excessively volatile boom-bust behavior of stock markets, we generalized the stock market model proposed by [10]. To be precise, we considered a trading environment in which market makers adjust stock prices with respect to the orders placed by chartists, fundamentalists, and sentiment traders. As usual, chartists place buying orders when the stock price increases and selling orders when it decreases. In contrast, fundamentalists place buying orders when the stock market is undervalued and selling orders when it is overvalued. The order sizes of chartists and fundamentalists are proportional to their trading signals. Moreover, sentiment traders, being subject to animal spirits, display three generic sentiment states. Sentiment traders optimistically buy a certain amount of stocks when the stock market is sufficiently rising, pessimistically sell a certain amount of stocks when the stock market is sufficiently falling, and neutrally abstain from trading otherwise. Clearly, the stock market model proposed by [10] captures only two generic sentiment states, namely optimism and pessimism.

As it turns out, the generalized stock market model results in a 2D piecewise-linear map defined on three partitions with two discontinuity lines. We have shown that the model gives rise to coexisting attractors, since a locally stable fixed point, at which the stock price matches its fundamental value, may coexist with one or more attracting cycles, at which the stock price oscillates around its fundamental value. We have detected the border-collision bifurcation boundaries of the periodicity regions related to attracting cycles with rotation number $1/n$, $n \geq 3$, belonging to two different kinds of families, with points in two outermost partitions only and with points in all three partitions. These two kinds of families are infinitely many, and all issuing from the center bifurcation line at $b = 1$. We have shown numerical evidence that the corresponding periodicity regions are organized in two different period-adding bifurcation structures issuing from the points associated with rational rotation numbers. Moreover, the existence of the third (middle) partition leads also to new dynamic results in the phase plane structure associated with the center bifurcation. We have shown the existence of an invariant polygon or an invariant ellipse (associated with a rational or irrational rotation number, respectively) filled with periodic or quasiperiodic trajectories.

This kind of structure has not been observed in other maps so far and we emphasize that this is related to the map defined in three partitions (each reflecting a different generic sentiment state). For the original stock market model proposed by [10], in which sentiment traders are either optimistic or pessimistic, this cannot occur.

We have shown that for parameters in the stability box all the existing cycles are attracting, coexisting with the locally attracting fundamental fixed point, and the associated basins of attraction are separated by segments of the discontinuity lines and the related preimages. Knowledge of the properties of the basins of attraction of coexisting attractors is important from an economic policy perspective. To achieve efficient stock markets, policymakers may seek to influence the behavior of market participants, e.g., by imposing transaction taxes, or to take part in the trading process themselves, e.g., by offsetting orders placed by chartists, such that the size of the basin of attraction for which the stock price converges towards its fundamental value increases.

We have also shown that in our map, the 2-cycle is always a saddle when it exists, for parameters outside the stability box of the fixed point, when all the existing cycles are of saddle type. However, bounded dynamics can exist, leading to a chaotic attractor whose structure is similar to that of a Belykh map (the ω-limit set of the unstable set of the saddle 2-cycle). A chaotic attractor exists as long as the saddle 2-cycle is not homoclinic, and we have detected the homoclinic bifurcations curves, associated with the discontinuity lines (since the contact between the stable and unstable sets of the 2-cycle

may first occur with one or the other discontinuity), that lead to divergence of almost all trajectories in the phase plane. This region is also relevant in the applied context. Since these parameter combinations are located outside the stability box, implying divergent stock market dynamics in the absence of animal spirits, when fundamentalists trade quite aggressively there are instances where the behavior of sentiment traders lends the stock market at least some kind of stability. Overall, this testifies the intricateness of the functioning of stock markets.

We conclude our paper by pointing out a few avenues for future research. Note that our map is symmetric with respect to the origin. Hence, it may be worthwhile to consider asymmetric specifications of our stock market model, e.g., to assume that the buying behavior of optimistic sentiment traders is not exactly the opposite of the selling behavior of pessimistic ones. This may be achieved by introducing two autonomous demand parameters, say d_U and d_L, or by introducing two different threshold levels, say h_U and h_L. Moreover, it may also be worth considering the case $0 < d < h$. In fact, a preliminary investigation has shown that similarly to the case $0 < h < d$, there exists a region in the parameter space related to the coexistence of different attracting cycles, although, unlike the case considered in our paper, a larger region in which the fixed point is the unique attractor can exist as well. Needless to say, more work is required to better understand the behavior of piecewise-linear discontinuous maps and the functioning of stock markets.

Declaration of competing interest

The authors declare that they have no known competing financial interests or personal relationships that could have appeared to influence the work reported in this paper.

Data availability

No data was used for the research described in the article.

Acknowledgments

D. Radi and L. Gardini acknowledge financial support from the Czech Science Foundation (GACR) under project 23-06282S, and an SGS research project of VŠB-TUO, Czech Republic (SP2023/19). I. Sushko acknowledges a partial financial support by the NAS of Ukraine within the project “Mathematical modeling of complex dynamical systems and processes caused by the state security” (Reg. No. 0123U100853). She is also grateful to the University of Urbino, DESP, for the hospitality during her stay there as a visiting researcher.

References

[1] Dieci R, He X-Z. Heterogeneous agent models in finance. In: Hommes C, LeBaron B, editors. Handbook of computational economics: heterogeneous agent modeling. Amsterdam: North-Holland; 2018, p. 257–328.
[2] Westerhoff F, Franke R. Agent-based models for economic policy design: two illustrative examples. In: Chen S-H, Kaboudan M, Du Y-R, editors. The oxford handbook of computational economics and finance. Oxford: Oxford University Press; 2018, p. 520–58.
[3] Beja A, Goldman M. On the dynamic behaviour of prices in disequilibrium. J Finance 1980;34:235–47.
[4] Frankel J, Froot K. Understanding the U.S. dollar in the eighties: the expectations of chartists and fundamentalists. Econ Rec 1986;62:24–38.
[5] Brock W, Hommes C. Heterogeneous beliefs and routes to chaos in a simple asset pricing model. J Econom Dynam Control 1998;22:1235–74.
[6] Huang W, Day R. Chaotically switching bear and bull markets: the derivation of stock price distributions from behavioral rules. In: Day R, Chen P, editors. Nonlinear dynamics and evolutionary economics. Oxford: Oxford University Press; 1993, p. 169–82.
[7] Tramontana F, Westerhoff F, Gardini L. The bull and bear market model of Huang and day: Some extensions and new results. J Econom Dynam Control 2013;37:2351–70.
[8] Jungeilges J, Maklakova E, Perevalova T. Asset price dynamics in a bull and bear market. Struct Change Econ Dyn 2021;56:117–28.
[9] Anufriev M, Gardini L, Radi D. Chaos, border collisions and stylized empirical facts in an asset pricing model with heterogeneous agents. Nonlinear Dynam 2020;102:993–1017.
[10] Gardini L, Radi D, Schmitt N, Sushko I, Westerhoff F. Causes of fragile stock market stability. J Econ Behav Organ 2022;200:483–98.
[11] Campisi G, Panchuk A, Tramontana F. A discontinuous model of exchange rate dynamics with sentiment traders. Ann Oper Res 2023. http://dx.doi.org/10.1007/s10479-023-05387-2.
[12] Gardini L, Radi D, Schmitt N, Sushko I, Westerhoff F. Perception of fundamental values and financial market dynamics: Mathematical insights from a 2D piecewise-linear map. SIAM J Appl Dyn Syst 2022;21:2314–37.
[13] Zhusubaliyev ZhT, Mosekilde E. Bifurcations and chaos in piecewise-smooth dynamical systems. World Sci. Ser. Nonlinear Sci. Ser. A Monogr. Treatises, Vol. 44, Hackensack, NJ: World Scientific; 2003.
[14] di Bernardo M, Budd CJ, Champneys AR, Kowalczyk P. Piecewise-smooth dynamical systems: theory and applications. Appl. Math. Sci., Vol. 163, New York: Springer; 2008.
[15] Simpson D. Bifurcations in piecewise-smooth continuous systems. World scientific series on nonlinear science, Vol. 70, Singapore: World Scientific; 2010.
[16] Puu T, Sushko I. Business cycle dynamics: models and tools. NY: Springer-Verlag; 2006.
[17] Nusse HE, Yorke JA. Border-collision bifurcations including ‘period two to period three’ bifurcation for piecewise smooth systems. Physica D 1992;57:39–57.
[18] Nusse HE, Yorke JA. Border-collision bifurcations for piecewise smooth one dimensional maps. Int J Bifurcation Chaos 1995;5:189–207.
[19] Avrutin V, Gardini L, Sushko I, Tramontana F. Continuous and discontinuous piecewise-smooth one-dimensional maps: invariant sets and bifurcation structures. Singapore: World Scientific; 2019.
[20] Rakshit B, Apratim M, Banerjee S. Bifurcation phenomena in two-dimensional piecewise smooth discontinuous maps. Chaos 2010;20:033101.
[21] Mira C. Embedding of a Dim1 piecewise continuous and linear leonov map into a Dim2 invertible map. In: Global analysis of dynamic models for economics, finance and social sciences. New York: Springer; 2013, p. 337–68.
[22] Simpson D. Unfolding codimension-two subsumed homoclinic connections in two-dimensional piecewise-linear maps. Int J Bifurcation Chaos 2020;30(3):2030006.
[23] Simpson D, Meiss J. Neimark-Sacker bifurcations in planar, piecewise-smooth, continuous maps. SIAM J Appl Dyn Syst 2008;7:795–824.
[24] Sushko I, Gardini L, Matsuyama K. Dynamics of a generalized fashion cycle model. Chaos Solitons Fractals 2019;126:135–47.
[25] Sushko I, Gardini L. Center bifurcation for two-dimensional border-collision normal form. Int J Bifurcation Chaos 2008;18:1029–50.
[26] Keener JP. Chaotic behavior in piecewise continuous difference equations. Trans Amer Math Soc 1980;261(2):589–604.
[27] Belykh V, Belykh I. Belykh map. Scholarpedia 2011;6(10):5545.
[28] Keynes JM. The general theory of employment, interest and money. London: Macmillan; 1936.
[29] Sushko I, Gardini L. Degenerate bifurcations and border collisions in piecewise smooth 1D and 2D maps. Int J Bifurcation Chaos 2010;20:2045–70.
[30] Milnor J. On the concept of attractor. Comm Math Phys 1985;99:177–95.
[31] Mira C, Gardini L, Barugola A, Cathala JC. Chaotic dynamics in two-dimensional noninvertible maps. Singapore: World Scientific; 1996.
[32] Belykh V, Barabash N, Grechko D. Existence proofs for strange attractors in piecewise-smooth nonlinear Lozi-Henon and Belykh maps. J Difference Equ Appl 2023;1–21. http://dx.doi.org/10.1080/10236198.2023.2193653.